Co-crystallization induced spontaneous deracemization: A general innovative thermodynamic approach to deracemization.

Michael Guillot‡*, Joséphine de Meester‡, Sarah Huynen‡, Laurent Collard‡, Koen Robeyns‡, Olivier Riant‡, Tom Leyssens‡*.

‡Institute of Condensed Matter and Nanosciences, Université Catholique de Louvain, Louvain-La-Neuve, Belgium.

Supporting Information Placeholder

ABSTRACT: Processes leading to enantiopure compounds are of utmost importance, in particular for the pharmaceutical industry. Starting from a racemic mixture, Crystallization Induced Diastereomeric Transformation allows for a theoretical 100% transformation of the desired enantiomer. However, this method has the inherent limiting requirement for the organic compound to form a salt. In this contribution, this limitation is lifted by introducing co-crystallization in the context of thermodynamic deracemization, with the process applied to a model chiral fungicide. We here report a new general single thermodynamic deracemization process based on co-crystallization for the deracemization of (R,S)-4,4-dimethyl-1-(4-fluorophenyl)-2-(1H-1,2,4-triazol-1-yl)-Pentan-3-one. This work presents the feasibility of this novel approach and paves the way to further development of such processes.

With the increasing number of enantiopure chiral drugs developed every year[1] and regulatory instances encouraging the development of enantiopure compounds[2], processes allowing access to these, are of utmost importance. In spite of significant advances in asymmetric synthesis (in particular asymmetric catalysis), the most prominent way to enantiopure drugs nowadays still involves formation of a racemic compound[3] and separation of the unwanted enantiomer through a resolution process[4-8], or its transformation into the desired enantiomer, in a so-called deracemization process. Crystallization-based resolution processes are less costly than eg. chromatographically based techniques and therefore industrially wide-spread. Typical crystallization based resolution processes are preferential crystallization[9-11] and diastereomeric resolution.[12-14] Going beyond separation, crystallization based deracemization processes aim at transforming the unwanted enantiomer (distomer) into the desired one (eutomer). Over the recent years, different deracemization tools were developed. The kinetic process of Viedma Ripening (VR) [15,16] and Dynamic Preferential Crystallization (DPC) [17] require a conglomerate forming racemate and are therefore inherently limited to 5-10% of all compounds. Crystallization Induced Diastereomeric Transformation--CDIT[18,19] , on the other hand, is a thermodynamical approach, based on the differences in solubility between two diastereomeric salts and does therefore not require the formation of such a conglomerate.

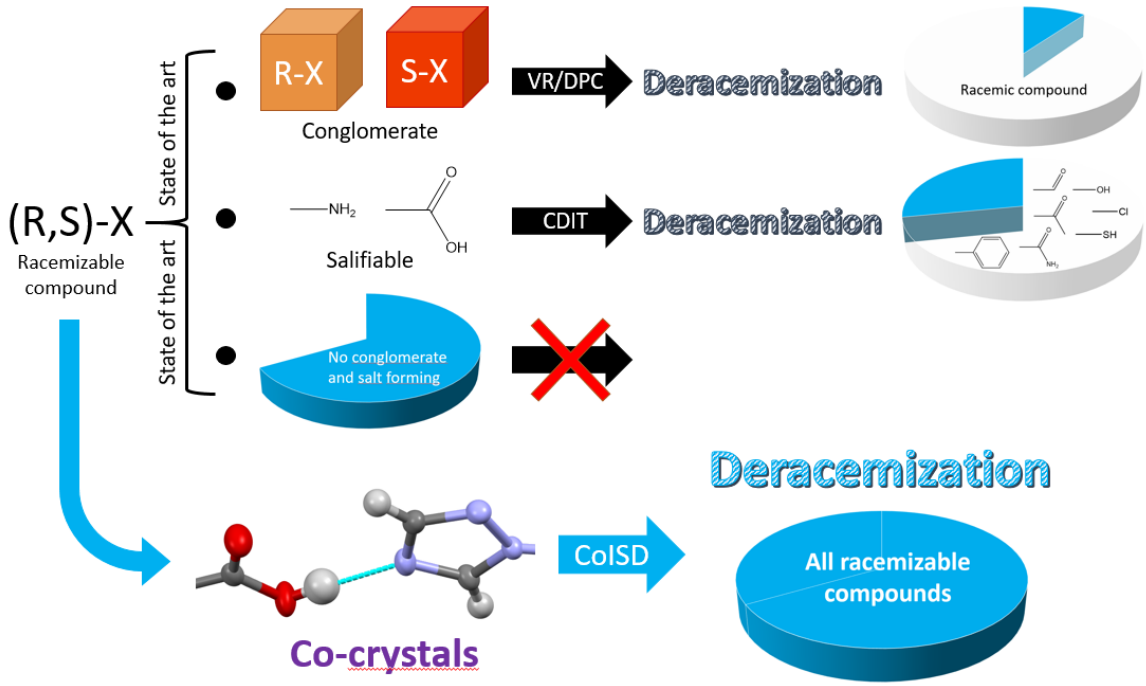

Scheme 1 State of the art regarding deracemization and how Co-crystallization induced spontaneous deracemization (CoISD) redistributes the cards and opens new possibilities in the world of deracemization.

As highlighted by a 2006 literature revue CDIT can only be performed on salt-forming compounds with the vast majority of studied systems combining a carboxylic acid with an amine[20]. For non-salifiable compounds, to the best of our knowledge, no thermodynamically based deracemization method has been reported and thus many racemizable compounds are left with no viable option for deracemization. We are the first, to introduce here such a method, based on co-crystallization, expanding the scope of thermodynamically based deracemization processes to all racemizable compounds (scheme 1). Co-crystallization typically relies on strong intermolecular interactions like hydrogen or halogen bonding[21], which are more universal. Co-crystallization was recently explored by us and others in the context of chiral resolution, targeting several racemic drug systems[22-25]. Based on these methods, and drawing a parallelism to CIDT, we set out to go beyond chiral resolution targeting a Co-crystallization Induced Spontaneous Deracemization (CoISD) process. The process developed here is innovative, industrially friendly and scope-expanding. It is a thermodynamic process applicable to all, non-salt as well as salt forming compounds, and both to conglomerate or racemic compound forming systems, hereby making it a general process compared to all the other crystallization based deracemization processes.

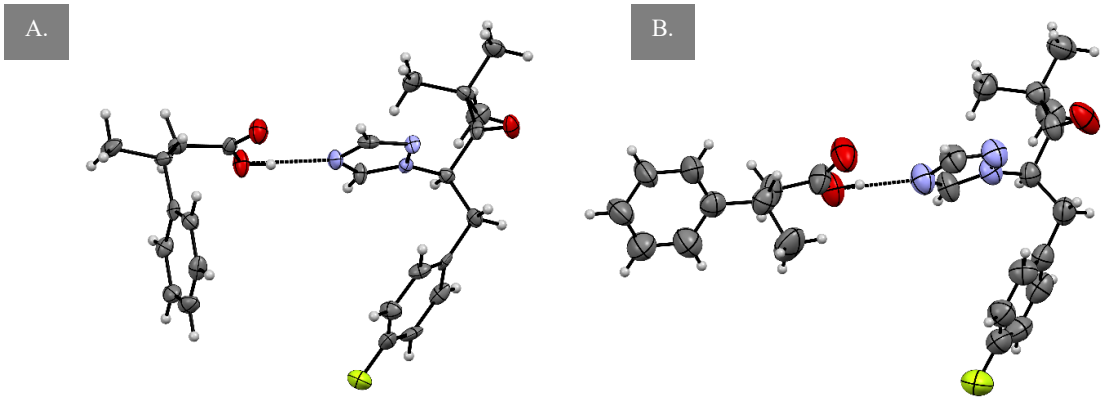

Figure 1. A. Asymmetric unit of the (S)- 4,4-dimethyl-1-(4-fluorophenyl)-2-(1H-1,2,4-triazol-1-yl)-Pentan-3-one-(S)-3-Phenylbutyric acid-co-crystal. B. Asymmetric unit of the (R)- 4,4-dimethyl-1-(4-fluorophenyl)-2-(1H-1,2,4-triazol-1-yl)-Pentan-3-one-(S)-3-Phenylbutyric acid-co-crystal. Displacement ellipsoids are drawn at the 50% probability level. Hydrogen bonds are shown as black dashed lines. Disorder is left out for clarity.

We used a model system to develop the CoISD process. The racemic target compound (R,S)-4,4-dimethyl-1-(4-fluorophenyl)-2-(1H-1,2,4-triazol-1-yl)-Pentan-3-one [RS-BnFTP] belongs to a family of fungicidal compounds[26], for which a conglomerate forming system has already successfully been deracemized through the kinetic Viedma ripening procedure.[27,28] Combining BnFTP with the chiral co-former, S-3-Phenylbutyric acid (S-PBA), a diastereomeric pair of co-crystals can be obtained. Each diastereomer crystallizes in a chiral space group with the asymmetric unit only containing one enantiomer of the target compound alongside S-PBA[23,25,29]. The diastereomers crystallize in the $P2_12_12_1$ and $P2_1$ space groups for [(S)-BnFTP-(S)-3-Phenylbutyric acid] (fig. 1.A) and [(R)-BnFTP-(S)-3-Phenylbutyric acid] (Fig. 1.B) respectively. The former will be referred to as the (S,S)-co-crystal and is the energetically favored diastereomer[1]. As a consequence, this diastereomer has a lower solubility compared to the (R,S)-co-crystal.

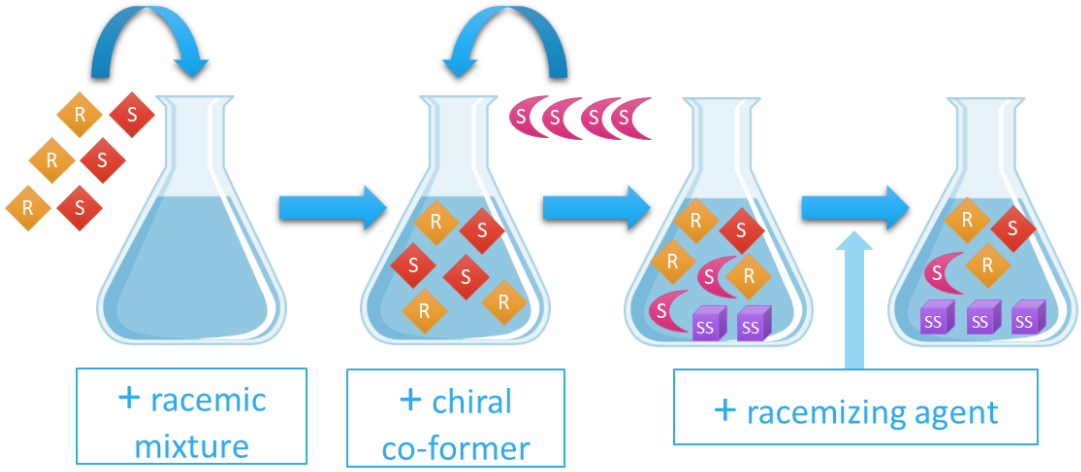

Scheme 2 Principle of the Cocrystallization Induced Spontaneous Deracemization process.

[1] When mixing both racemic RS-BnFTP and RS-PBA a mixture of the (R,R) and (S,S) co-crystals are formed instead of the (R,S) – (S,R) mixture, showing a higher stability of the (S,S) with respect to the (R,S) diasteriomer.

The principle behind CoISD (Scheme 2) taps into this solubility difference.[30] Given the right conditions addition of S-PBA to a racemic mixture of BnFTP will selectively lead to crystallization of only the (S,S)-cocrystal (purple cubes). This induces a solution enantiomeric excess towards R-BnFTP (orange squares). Addition of a racemizing agent will pull the solution imbalance towards the racemic equilibrium once more, implying a net transformation in solution of R-BnFTP to S-BnFTP. The associated concentration increase in S-BnFTP will lead to a solution that is supersaturated with respect to the (S,S)-cocrystal[2], which continues to crystallize as long as a sufficient amount of co-former is present in solution. This process is purely thermodynamic and eventually leads to spontaneous full deracemization[3].

Toluene was selected as crystallization solvent, as the (S,S)-cocrystal behaves congruently in this solvent and furthermore shows low solubility. On top, this solvent allows the BnFTP racemization reaction to run without major difficulty. Moreover, there is a substantial solubility difference between both diastereomers. Chiral resolution conditions in toluene (SI), allow to crystallize the (S,S)-cocrystal with a 32% yield[4] and an ee of 98.6% (Fig. 2) starting from the RS-BnFTP racemate. This process leaves a solution imbalance in favor of R-BnFTP (ee=58.6%).

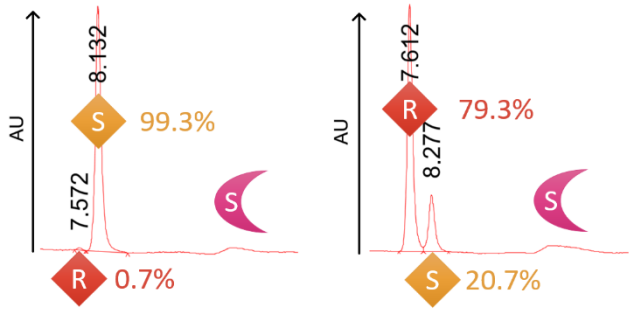

Figure 2. (a) Chiral chromatography of the cake (b) and the filtrate obtained from the RS-BnFTP chiral resolution process in toluene.

Besides induction of a solution enantiomeric imbalance, a racemization reaction is also a prerequisite for the development of a deracemization process. In our case, racemization is based on the keto-enol equilibrium of BnFTP using either a Brønsted acid or base.[31] BnFTP racemizes freely in the presence of weak bases but does not in presence of weak or strong acids. 1,8-diazabicyclo[5.4.0]undec-7-ene (DBU) was chosen as the racemizing agent since the use of one equivalent of DBU at room temperature led to full racemization in 30 minutes, whereas a 5 mol% catalytic amount of DBU was shown to induce complete racemization in 6h (SI). Unfortunately, addition of the base to a solution containing both BnFTP and co-former no longer led to racemization at this temperature. This can easily be understood, as DBU (less than 1eq with respect to BnFTP and co-former) will deprotonate the carboxylic acid of the coformer, producing a much weaker carboxylate base. This latter is not strong enough to induce racemization under the initial conditions studied. A similar situation is often encountered in CDIT-processes for which a temperature increase is typically required for the racemization to occur.[32,33] Keeping this in mind, we performed racemization in presence of the coformer (and sub-stoichiometric amounts of DBU) at higher temperatures. After 12 hours at 110°C, the filtrate obtained from the resolution fully racemized while 2h at 90°C partially racemized it. Temperature increases are usually counterproductive with respect to crystallization processes. To allow for a reasonable yield, we decided to physically separate both processes working with a crystallization vessel at 10°C and a racemization vessel at 90°C.[5] The liquid from the crystallization vessel with an enantiomeric imbalance in favor of the distomer is continuously transferred to the racemization vessel, and the racemic solution from the racemization to the crystallization vessel, as shown in Fig. 3. A 3D representation of the system is given in Fig. 4.

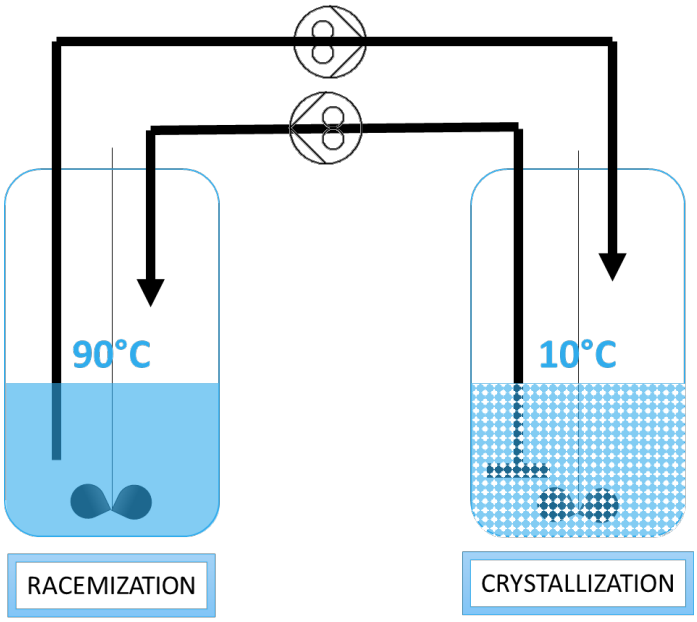

Figure 3. Sketch of the single process deracemization process set-up.

[2] The co-crystal solubility product depends on the concentration of both components in solution K_{sp}= [S-BnFTP]*[(S)-PBA]

[3] Full deracemization does not imply a 100% transformation of R into S. The final solution (in equilibrium with the enantiopure solid state) still contains a mixture of R- and S-BnFTP. The lower the solubility of the co-crystal, the higher the overall deracemization.

[4] It must be noted that the maximum yield for a resolution is 50%

[5] For a process which does not require high temperatures, a one-pot method combining crystallization and racemization is fully achievable.

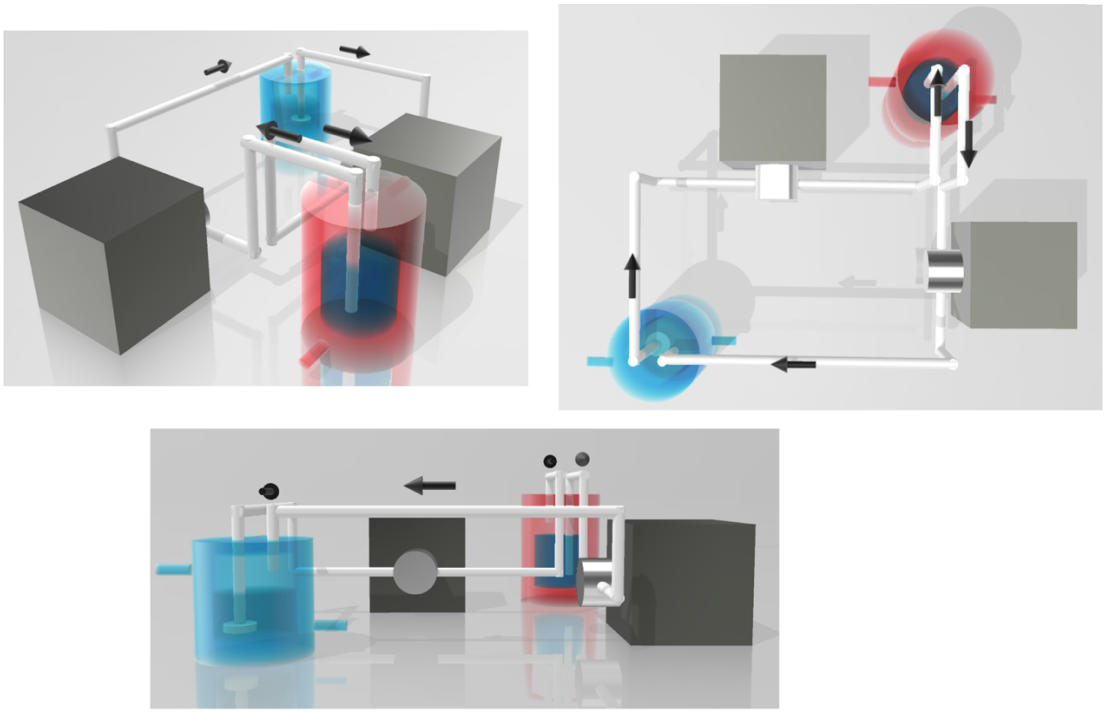

Figure 4. 3D representation of the deracemization system set-up. Liquids are continuously pumped between the crystallization (blue) and racemization (red) vessel.

In this paper, we pioneer in showing the success of the CoISD process through 3 experiments. Each experiments is performed using a 1 equivalent mixture of RS-BnFTP and co-former and 7.5% mol of DBU. After each experiment, the solid in suspension was filtered and the cake washed with toluene (SI). Tubing and reactor vessels were flushed with acetone, and solutions added to the filtrate. This latter was evaporated and the weight of the cake and solid recovered from the filtrate were determined. Both were further analyzed by chiral HPLC to check the ratio of R vs. S-BnFTP. Combining these measurements allowed for a full mass balance. Results are given in table 1. In all cases, the cake was found to be enantiopure. Expectedly, starting with the S-coformer leads to crystallization of S-BnFTP while the R enantiomer can be crystallized using the co-former of opposite handedness. Experiment 1, led to a recovered yield of over 50%, inherently implying that we went beyond mere resolution (max. yield of 50%). The full mass balance, showed a deracemization to have occurred (bold numbers) for all experiments as can be observed by looking at the total R/S ratio at the end of the experiments, with in the case of experiment 2, the 50/50 R/S mixture being thermodynamically transformed into a 87/13 mixture. From the follow-up of experiment 2 (SI), racemization kinetics were shown faster than crystallization kinetics. For this reason, heating was decreased for the third experiment with racemization becoming the limiting factor, yielding less deracemization over the same period of time. With these 3 experiments, we are the first to demonstrate that deracemization can be thermodynamically induced to yield enantiopure co-crystalline solid with high purity. Depending on the co-former's handedness used, one can select the desired enantiomer. As both racemization and crystallization kinetics interplay, developing an optimized process requires future optimization of all process parameters.

Experiment	C(BnFTP-PBA)	V_{DBU} / %mol	Yield[6] (cake)	ee_{cake}	$ee_{filtrate}$	Ratio R/S total	$T_{rac.}$	runtime
1 (S-PBA)	0.20 mol/L	203µL / 7.5%	50.7%	0.999 [S]	0.276 [S]	**18/82**	90°C	4 days
2 (R-PBA)	0.25 mol/L	254µL / 7.5%	44.6%	1.00 [R]	0.54 [R]	**87/13**	90°C	5 days
3 (R-PBA)	0.30 mol/L	305µL / 7.5%	38.7%	0.97 [R]	0.246 [S]	**38/62**	75°C	5 days

Table 1 Key parameters and results for each of the three deracemization experiments. For each experiment, the same volume of toluene was used, 90mL. For the enantiomeric excess (ee), the enantiomer in excess is given in brackets. Yield is calculated with respect to the total mass retrieved at the end of the experiment.

[6] It must be noted that both experiment 1 and 2 did not reach crystallization equilibrium before filtration and thermodynamic yields are expected to be higher. Before filtration, it would be advisable to leave the process enough time to equilibrate.

In conclusion, we report an innovative thermodynamic deracemization process coupling selective co-crystallization to a racemization reaction. We successfully deracemized RS-BnFTP targeting either the S- or R-enantiomer based on choice of the co-former handedness. Unlike kinetic processes such as Viedma Ripening or dynamic preferential crystallization, CoISD can target conglomerate as well as racemic compounds, and contrary to CDIT, CoISD can be used for those compounds that do not form salts. Overall this makes CoISD a general deracemization process, which in the future we will likely see applied to a multitude of compounds. Further studies are currently ongoing to optimize the process parameters and understand underlying racemization and crystallization kinetics.

ASSOCIATED CONTENT

Supporting Information

This material is available free of charge via the Internet at http://pubs.acs.org/.
The material and methods can be found in this section alongside some tables displaying all the results of the different experiments conducted. CCDC 1984002-1984003 contain the supplementary crystallographic data for this paper. The data can be obtained free of charge from The Cambridge Crystallographic Data Centre via www.ccdc.cam.ac.uk/structures

AUTHOR INFORMATION

Corresponding Author

*E-mail: michael.guillot@uclouvain.be. Web: https://uclouvain.be/fr/repertoires/michael.guillot.
*E-mail: tom.leyssens@uclouvain.be. Web: https://uclouvain.be/fr/repertoires/tom.leyssens

Notes

The authors declare no competing financial interests.

ACKNOWLEDGMENT

The authors would like to thank the UCL and FNRS for financial support. The authors would also like to thank the FNRS (PDR T.0149.19 – M. Guillot is a FRIA research fellow) for financial support.

REFERENCES

[1] Murakami H. From Racemates to Single Enantiomers – Chiral Synthetic Drugs over the last 20 Years. In: Novel Optical Resolution Technologies. Heidelberg: Springer, **2006**: 274-278. Available at: https://link.springer.com/content/pdf/10.1007%2F978-3-540-46320-7.pdf. Accessed September 5, 2018.

[2] Administration F.D. **1992**. Available at: www.fda.gov/Drugs/GuidanceComplianceRegulatorylnformation/Guidances/ucm122883.htm**.** Accessed September 5, 2018.

[3] Calcaterra, A.; D'Acquarica, I. *J Pharm Biomed Anal.* **2018,** 147, 323–340.

[4] Xie, R.; Chu, L.-Y.; Deng, J.-G. *Chem. Soc. Rev*. **2008**, 37, 1243-1263

[5] Whitesell, J. K.; Reynolds, D. *J. Org. Chem*. **1983**, 48, 20, 3548-3551.

[6] Xie, S.-M.; Zhang, Z.-J.; Wang, Z.-Y.; Yuan, L.-M. *J. Am. Chem. Soc*. **2011**, 133, 31, 11892-11895.

[7] Noorduin, W. L.; van der Asdonk, P.; Meekes, H.; van Enckevort, W. J. P.; Kaptein, B.; Leeman, M.; Kellogg, R. M.; Vlieg, E. *Angew. Chem. Int. Ed*. **2009**,48, 3278 –3280.

[8] Okamoto, Y.; Ikai, T. *Chem. Soc. Rev*. **2008**, 37, 2593-2608.

[9] Coquerel G. Preferential Crystallization. In: Novel Optical Resolution Technologies. Heidelberg: Springer, **2006**: 4-18. Available at: https://link.springer.com/content/pdf/10.1007%2F978-3-540-46320-7.pdf. Accessed September 5, 2018.

[10] Levilain, G., & Coquerel, G. *CrystEngComm*. **2010**, 12(7), 1983-1992.

[11] Rougeot, C., & Hein, J. E. *Org. Process Res. Dev*. **2015**, 19(12), 1809-1819.

[12]Kozma, D. CRC handbook of optical resolutions via diastereomeric salt formation. CRC Press, **2001**.

[13] Marchand, P., Querniard, F., Cardinaël, P., Perez, G., Counioux, J. J.; Coquerel, G. *Tetrahedron-Asymmetry*. **2004**, 15(16), 2455-2465.

[14] He, Q., Peng, Y. F., & Rohani, S. *Chirality*. **2010**, 22(1), 16-23.

[15] Sögütoglu, L.-C.; Steendam, R.R. E.; Meekes, H.; Vlieg, E.; Rutjes, F. P. J. T. *Chem. Soc. Rev*. **2015**, 44, 6723-6732.

[16] Viedma, C. *Phys. Rev. Lett*. **2005**, 94,3−6.

[17] Sakamoto, M.; Mino, T. Total Resolution of Racemates by Dynamic Preferential Crystallization. In: Tamura R., Miyata M. (eds) Advances in Organic Crystal Chemistry. Tokyo: Springer, **2015**.

[18] Toda, F.; Tanaka, K. *Chem. Lett*. **1983**, 661.

[19] Hassan, N. A.; Bayer, E.; Jochims, J. C. *J. Chem. Soc.***1998**, 3747.

[20] Brands, K. M. J.; Davies, A. *J. Chem. Rev.* **2006**, 106 (7), 2711–2733.

[21] Andrew D. Bond. *Cryst. Eng. Comm*. **2007**, 9, 833–834.

[22] Thorey, P.; Bombicz, P.; Szilágyi, I. M.; Molnár, P.; Bánsághi, G.; Székely, E.; Simándi, B.; Párkányi, L.; Pokol, G.; Madarász, J. *Thermochim. Acta*. **2010**, 497, 129–136.

[23] Sanchez-Guadarrama, O.; Mendoza-Navarro, F.; Cedillo-Cruz, A.; Jung-Cook, H.; Arenas-García, J. I.; Delgado-Díaz, A.; Herrera-Ruiz, D.; Morales-Rojas, H.; Hopfl. H. *Cryst. Growth Des*. **2016**, 16, 307−314.

[24] Springuel, G.; Norberg, B.; Robeyns, K.; Wouters, J.; Leyssens, T. *Cryst. Growth. Des*. **2012**, 12(1), 475-484.

[25] Springuel, G.; Leyssens, T. *Cryst. Growth Des*. 2012, 12 (7), 3374–3378.

[26] Balasubramanyan, S. (1981). Fungicidal compounds. US4243405A.

[27] Suwannasang, K.; Flood, A.E.; Rougeot, C.; Coquerel, G. *Cryst. Growth Des*. **2013**, 13, 3498-3504.

[28] Rougeot, C.; Guillen, F.; Plaquevent, J.C.; Coquerel, *G. Cryst. Growth Des*. **2015**, 15, 2151-2155.

[29] Habgood, M. *Cryst. Growth Des.* **2013**, 13 (10), 4549–4558.

[30] Lam, A. W. H. and Ng, K. M. *AlChE J*. **2007**, 53, 429-437.

[31] Reusch W.; Farmer S. **2015**. Available at: https://chem.libretexts.org/Textbook_Maps/Organic_Chemistry/Supplemental_Modules_(Organic_Chemistry)/Reactions/Rearrangement_Reactions/Keto-Enol_Tautomerism. Accessed September 10, 2018.

[32] Davidson, E. M.; Turner, E. E. *J. Chem. Soc*. **1945**, 843.

[33] Shiraiwa, T.; Furukawa, T.; Tsuchida, S.; Sakata, M.; Sunami, M.; Kurokawa, H. Bull. *Chem. Soc. Jpn*. **1991**, 64, 3729.

Supporting Information:

1. The studied system

1.1 S/R-3-phenylbutyric acid

S/R-3-phenylbutyric acid was obtained from (RS)-3-Phenylbutyric acid (Sigma-Aldrich) carrying out a diastereomeric salt resolution. Resolution was carried out with the following protocol:

A 175g/L solution of (RS)-3-Phenylbutyric acid and S-1-phenylethylamine (1 equivalent of each, $m_{Phenylbutyric\ acid}$ = 20.13g; $m_{phenylethylamine}$ = 14.86g) was stirred in 200mL of a 1:3 ethanol/Toluene solvent mixture overnight at room temperature and yielded post filtration 13.24g of S-S salt with an enantiomeric excess of 0.41. This salt is then stirred overnight in 90mL of a 1:3 ethanol/Toluene solvent mixture at room temperature and filtrated to yield 7.64g of S-S salt with an enantiomeric excess of 0.91. This salt is again stirred overnight at room temperature in 35mL of a 1:3 ethanol/Toluene solvent mixture and filtrated to yield 6.23g of S-S salt with an enantiomeric excess of 0.98 (yield = 18%).

The same protocol was applied to obtain the R-3-phenylbutyric acid.

At each crystallization, the cake enantiopurity was analyzed by polarimetry with Anton Paar polarimeter at 589nm and 20°C in order to obtain the enantiomeric excess of the salt. Each calculation was done according to the following reasoning:

Phenylbutyric acid was shortened as PBA and Phenylethylamine as PEA. The "+" stand for the protonated PEA while the "-" stands for the deprotonated PBA.

M_{PEA+} = 122,18g/mol ; x_m^{PEA+} = 0.428

M_{PBA-} = 163,2g/mol ; x_m^{PBA-} = 0.572

$$100\alpha = [\alpha]^{SPEA+} l c_m x_m^{PEA+} + [\alpha]^{SPBA-} l c_m x_m^{SPBA-} E$$

For an equimolar mixture of PEA+ et PBA- with a mass concentration of $c_m \in [10\ ;10{,}07 g/L]$

$[\alpha]^{SPEA+}$ was determinated in Ethanol with an equimolar mixture of SPEA and racemic PBA (E=0):

α = -0,068; c_m = 10,045g/L gives $[\alpha]^{SPEA+}$ = -15.81°

$[\alpha]^{SPBA-}$ was determinated in Ethanol with an equimolar mixture of SPEA and SPBA (E=1):

α = 0,091; c_m = 10,07g/L gives $[\alpha]^{SPBA-}$ = 27.64°

The enantiomeric excess of each SPEA sample was calculated with the following formula:

$$E = \frac{100\alpha - [\alpha]^{SPEA+} l c_m x_m^{PEA+}}{[\alpha]^{SPBA-} l c_m x_m^{SPBA-}}$$

The enantiomeric excess of each RPEA sample was calculated with the following formula:

$$E = -\frac{100\alpha + [\alpha]^{SPEA+} l c_m x_m^{PEA+}}{[\alpha]^{SPBA-} l c_m x_m^{SPBA-}}$$

All samples concentrations were comprised between 10g/L and 10,07g/L and all samples were an equimolar mixture of PEA and PBA.

1.2 (RS)-4,4-dimethyl-1-(4-fluorophenyl)-2-(1H-1,2,4-triazol-1-yl)-Pentan-3-one (RS-BnFTP)

RS-BnFTP was synthetized in 2 steps:

- **3,3-dimethyl-1-(1H-1,2,4-triazol-1-yl)- Butan-2-one (TP)**. 5.13g of 1,2,4 Triazol, 11g of Chloropinacolone (1.1eq) and 10.27g of K_2CO3 (1.5 eq) were added in 100mL of Acetonitrile. The mixture was stirred under reflux for 8h30. The mixture was filtered and the solvent was removed under vacuum. Then, 20mL of water were added and the residue was extracted with 50mL ethyl acetate, 3 times. The organics layers were combined, dried over $MgSO_4$, filtered and concentrated under vacuum. The crude was purified adding 10mL of diethyl ether and the mixture was stirred at room temperature for 5-6h in a closed round-bottom flask. Then, the mixture was filtered and a white solid recovered. The solid was dried at room temperature for 24h then weighed. 10.404g (84%) were obtained. mp = 67.2°C, R_f= 0.1 (1:1 EA/PE) Vanillin revelation (white spot), ^{1}H NMR (300 MHz, $CDCl_3$) δ (ppm): 1.11 (s, 9H, $C(CH_3)_3$), 5.11 (s,2H, N-CH_2-C=O), 7.77 (s, 1H, N=CH-N) 8.02 (s, 1H, N=CH-N). ^{13}C NMR (75 MHz, $CDCl_3$) δ (ppm): 26.43 ($C(CH_3)_3$), 43.88 ($C(CH_3)_3$), 53.52 (N-CH_2-C=O), 145.06 & 152.10 (N=CH-N), 206.51 (C=O).

- **4,4-dimethyl-1-(4-fluorophenyl)-2-(1H-1,2,4-triazol-1-yl)-Pentan-3-one (BnFTP).** 2g of TP, dissolved in 10mL of anhydrous DMF, were added dropwise at 0°C to a stirred suspension of 0.480g NaH (60% dispersion in mineral oil, 1eq) in 5mL of anhydrous DMF. Once, all the TP was added, 2826µL of p-fluorobenzyl chloride (2eq) were added at 0°C. Then, the mixture was warmed up to room temperature and left to react for 3h30. 10mL of water were added to quench the reaction. Then, 25mL ethyl acetate were added to perform a liquid-liquid extraction (3x). The organic layers were combined and dried over $MgSO_4$, filtered and concentrated under a strong vacuum to remove the remaining DMF. The crude was purified by column chromatography (Packing: PE pure, Eluent: 20:80 (EA:PE) till the compound starts coming out, then 50:50). 2.347g (71%) of a white solid was obtained after removal of all traces of solvent and recrystallization in toluene at RT<20°C. mp = 47.3°C, R_f= 0.58 (1:1 EA/PE) UV revelation + Vanillin (whitish spot), ^{1}H NMR (300 MHz, $CDCl_3$) δ (ppm): 1.00 (s, 9H, C(C**H**$_3$)$_3$), 3.19 (dd, 1H, J = 13.7, 7.7 Hz, CH-C**H$_a$**H$_b$-C$_{Ar}$), 3.34 (dd, 1H, J = 13.7, 7.7 Hz, CH-CH$_a$**H$_b$**- Car), 5.67 (t, 1H, J = 7.7 Hz, CH$_2$-C**H**-C=O), 6.90-6.97 (m, 2H, C$_{Ar}$=C$_{Ar}$**H**-C$_{Ar}$F), 7.02 (dtt, 2H, , J = 8.2, 5.2, 2.5 Hz, C$_{Ar}$=C$_{Ar}$**H**-C$_{Ar}$H), 7.87 (s, 1H, N=C**H**-N), 8.23 (s, 1H, N=C**H**-N). ^{13}C NMR (75 MHz, $CDCl_3$) δ (ppm): 25.77 (C(**C**H$_3$)$_3$), 38.82 (CH-**C**H$_2$-C$_{Ar}$) 45.19 (**C**(CH$_3$)$_3$), 63.04 (CH$_2$-**C**H-C=O), 115.95-116.24 (d, J = 21.44 Hz, **C$_{Ar}$**H), 131.01-131.12 (d, J = 8.22 Hz, **C$_{Ar}$**H), 131.12-131.17 (d, J = 3.79 Hz, **C$_{Ar}$**), 142.52 & 151.53 (N=**C**H-N), 160.78-164.05 (d, J = 246.46 Hz, **C$_{Ar}$**F), 209.37 (C=O).^{19}F NMR (282 MHz, $CDCl_3$) δ (ppm): -114.67.

Chloropinacolone (Fluorochem), 1,2,4 Triazol (SAF), Anhydrous DMF (Sigma), p-fluorobenzyl chloride (Acros), NaH (Acros) were purchased from commercial sources and used as received. **Column chromatography** was performed using neutral alumina silica gel 60 Å (40-63 µm). **NMR spectra** were obtained on a 300 MHz spectrometer. Chemical shifts are reported in parts per million (ppm) and were normalized regarding the chemical shift of the peak of the deuterated solvent used. For the ^{1}H NMR spectra, the value of the different solvent used are the following: $CHCl_3$ 7.26ppm. For the ^{13}C NMR spectra, the value of the different solvent used are the following: $CHCl_3$ 77.36ppm. Multiplicities are abbreviated as follows: singlet (s), doublet (d), triplet (t), quartet (q) and multiplet (m). For the 19F NMR, the peak of the robe was automatically removed from the spectra.

1.3 DBU was used as bought (Sigma-Aldrich).

1.4 Toluene was used as received (VWR).

2. The co-crystals

2.1 Co-crystal screening

The co-crystal was first identified by grinding of the two component as part of a larger screening where RS-BnFTP was ground with around 40 different co-former, each in separate vials. Grinding was carried out in a RETSCH mixer mill MM 400 for 90 min with a beating frequency of 30 Hz. The ground mixture were then analyzed by Powder X-ray Diffraction (PXRD). Those measurements were performed with a Siemens D5000 diffractometer equipped with a Cu X-ray source operating at 40 kV and 40 mA and a secondary monochromator allowing the selection of the Kα radiation of Cu (λ = 1.5418 Å). A scanning range of 2θ values from 2° to 72° at a scan rate of 0.6° min−1 was applied. The chromatogram obtained is given in figure 1 and compared to those of the parent compounds.

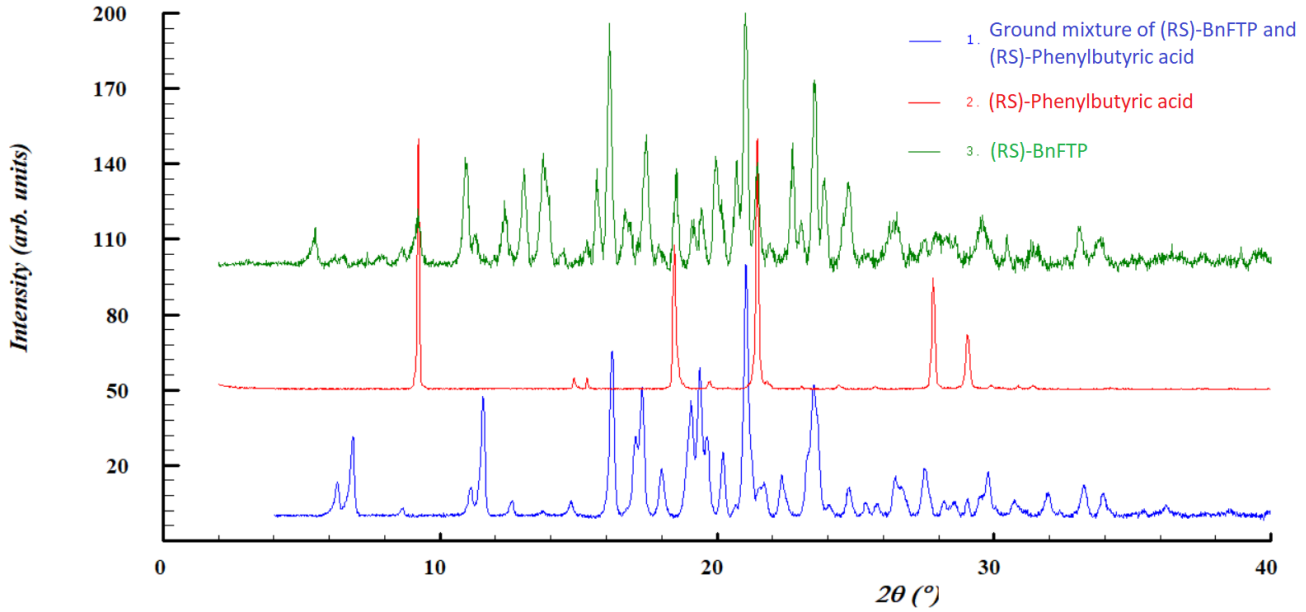

Figure 1 Diffractogram of the ground mixture of (R,S)-4,4-dimethyl-1-(4-fluorophenyl)-2-(1H-1,2,4-triazol-1-yl)-Pentan-3-one and (R,S)-3-phenylbutyric acid compared to the experimental diffractograms of both compounds alone.

2.2 Co-crystal structure

The **structure of both co-crystals** was determined by single crystal measurement. **For single crystal growth**, the (S,S) co-crystal was obtained from a cooling experiment in acetone (9°C) of a 1:1 mixture of (RS)-PBA and (RS)-BnFTP while the (R,S) co-crystal was obtained from solvent evaporation in ethyl acetate of a 1:1 mixture of a R-BnFTP and S-PBA. **Single Crystal-X-ray Diffraction (SC-XRD)** was performed on a Gemini Ultra R system (4-circle kappa platform, Ruby CCD detector) using Cu Kα radiation (λ = 1.54056 Å)/ or on a

MAR345 detector using monochromated Mo Kα radiation (λ = 0.71073 Å) (Xenocs Fox3D mirror) produced by a Rigaku UltraX 18 generator. The structures were solved by direct methods with SHELXS-97 and then refined on |F2| using SHELXL-97/or SHELXL2014. Non-hydrogen atoms were anisotropically refined and the hydrogen atoms (not implicated in H-bonds) in the riding mode with isotropic temperature factors fixed at 1.2 times U(eq) of the parent atoms (1.5 times for methyl groups). Hydrogen atoms implicated in H-bonds were localized in the Fourier difference maps (ΔF).

The crystal data and structure refinement are given in the two tables below.

Table 2 Crystal data and structure refinement for UCL896_mg_cpf12.

Identification code	mg_cpf12
Empirical formula	C25 H30 F N3 O3
Formula weight	439.52
Temperature	150(2) K
Wavelength	0.71073 Å
Crystal system	Orthorhombic
Space group	$P2_12_12_1$
Unit cell dimensions	a = 5.5481(4) Å a= 90°.
b = 16.4771(12) Å	b= 90°.
c = 25.6791(19) Å	g = 90°.
Volume	2347.5(3) $Å^3$
Z	4
Density (calculated)	1.244 Mg/m^3
Absorption coefficient	0.088 mm^{-1}
F(000)	936
Crystal size	0.42 x 0.03 x 0.02 mm^3
Theta range for data collection	2.938 to 23.248°.
Index ranges	-6<=h<=6, -18<=k<=18, -28<=l<=28
Reflections collected	13690
Independent reflections	3340 [R(int) = 0.1121]
Completeness to theta = 23.248°	99.5 %
Absorption correction	Semi-empirical from equivalents
Max. and min. transmission	1.00000 and 0.58890
Refinement method	Full-matrix least-squares on F^2
Data / restraints / parameters	3340 / 0 / 294
Goodness-of-fit on F^2	1.098
Final R indices [I>2sigma(I)]	R1 = 0.0837, wR2 = 0.1152
R indices (all data)	R1 = 0.1115, wR2 = 0.1236
Absolute structure parameter	2.1(10)
Extinction coefficient	n/a
Largest diff. peak and hole	0.198 and -0.188 $e.Å^{-3}$

Table 3 Crystal data and structure refinement for UCL1010_mg_compB.

Identification code	mg_compB	
Empirical formula	C25 H30 F N3 O3	
Formula weight	439.52	
Temperature	297(2) K	
Wavelength	0.71073 Å	
Crystal system	Monoclinic	
Space group	$P2_1$	
Unit cell dimensions	a = 5.7163(7) Å	a= 90°.
	b = 15.9831(18) Å	b= 98.507(12)°.
	c = 13.7113(15) Å	g = 90°.
Volume	1238.9(2) $Å^3$	
Z	2	
Density (calculated)	1.178 Mg/m^3	
Absorption coefficient	0.083 mm^{-1}	
F(000)	468	
Crystal size	0.50 x 0.50 x 0.07 mm^3	
Theta range for data collection	3.264 to 25.242°.	
Index ranges	-6<=h<=6, -19<=k<=19, -16<=l<=16	
Reflections collected	6625	
Independent reflections	4294 [R(int) = 0.0489]	
Completeness to theta = 25.242°	99.0 %	
Absorption correction	Semi-empirical from equivalents	
Max. and min. transmission	1.00000 and 0.62605	
Refinement method	Full-matrix least-squares on F^2	
Data / restraints / parameters	4294 / 106 / 379	
Goodness-of-fit on F^2	1.070	
Final R indices [I>2sigma(I)]	R1 = 0.0510, wR2 = 0.1215	
R indices (all data)	R1 = 0.0701, wR2 = 0.1331	
Absolute structure parameter	0.1(9)	
Extinction coefficient	n/a	
Largest diff. peak and hole	0.120 and -0.127 $e.Å^{-3}$	

3. Chiral resolution

In a vial, 1g of (RS)-BnFTP, previously synthetized, was solubilized in 8 mL of Toluene. Then, 0.6g of (S)-3-Phenylbutyric acid was added and the mixture was stirred overnight with a magnetic stirrer. A white solid in suspension was obtained. The mixture was filtered over Buchner and washed with cyclohexane. The solid was dried at 50°C for 2h. The cake was analyzed by chiral HPLC to determine its enantiomeric ratio. The filtrate was evaporated and analyzed by chiral HPLC. The **Chiral HPLC** set-up is the following: the pump is a Waters 600, the auto-sampler is a Waters 717 and the detector is a Waters 996. The column used is a Chiral Pak 1B chiral column with the following dimensions 250x4.6mm and a particle diameter of 5µm. The chromatograms were obtained from a detection at 254 nm. The mobile phase was 95% isohexane and 5% ethanol at a flow rate of 1 mL/min.

XRPD showed the recovered solid from the cake to the (S,S) co-crystal, matching the simulated pattern of the single crystal analysis. This allowed to attribute the HPLC peak belonging to the S-enantiomer of the target compound. As expected the R-enantiomer indeed showed a higher presence in the filtrate.

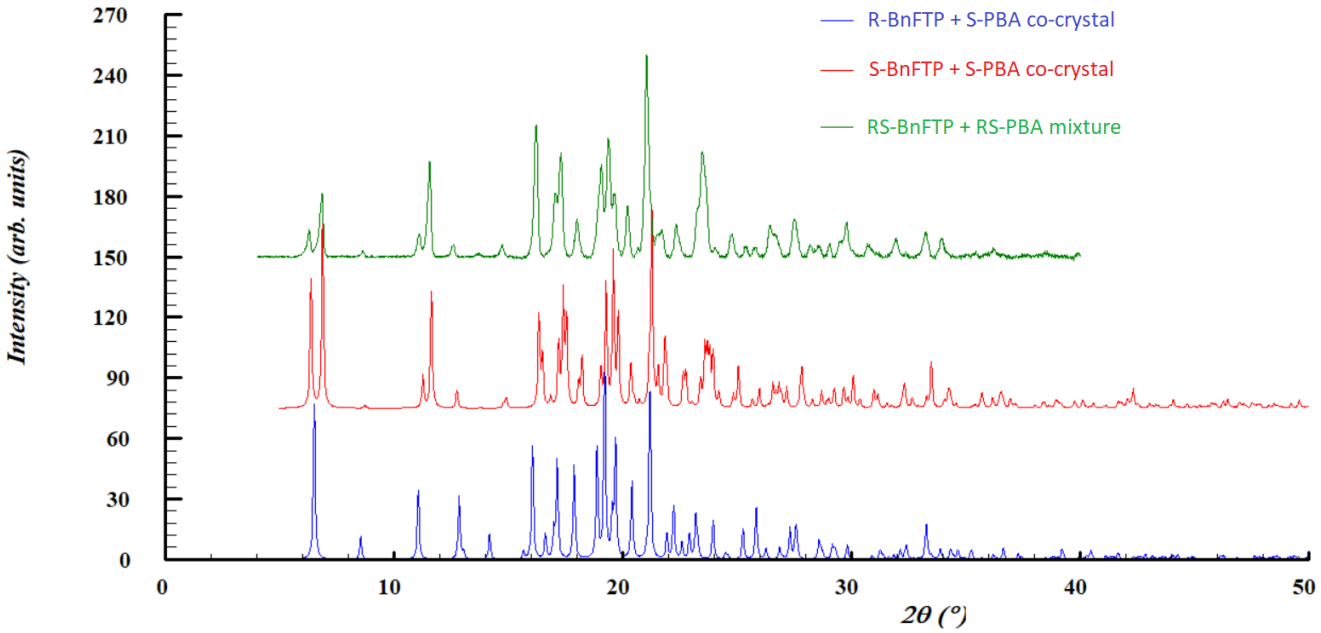

Figure 2 Diffractogram displaying the simulated pattern of both co-crystals compared to the physical mixture of RS-BnFTP and RS-PBA.

The chromatograms shows the signal of (S)-3-phenylbutyric acid trailing the signal from R-BnFTP. This is due to the fact that the acid tends to lag behind because of an equilibrium with the carboxylate occurring within the stationary phase. Despite this, the analysis of the chromatogram could still be carried out as figure 4 in the main text shows.

4. Deracemization process

4.1 Technical details of the set-up

The developed system uses two double-jacket vessels, one with a 10°C cooling liquid circulating through and the other with a 90°C heating liquid. Two gear pumps are used, one transferring liquid from the crystallization vessel to the racemization vessel, and one pump doing the opposite. A filter was used to avoid solid transfer occurring between the crystallization vessel and the racemization vessel. PTFE tubing used are toluene resistant. Stirring was carried out magnetically with a bottom stirrer in each vessel. The processes were carried out in a semi-continuous fashion: Over-night transfer of liquid between vessels was stopped. For the first two experiments, heating was maintained during the night while this was not the case for the third experiment.

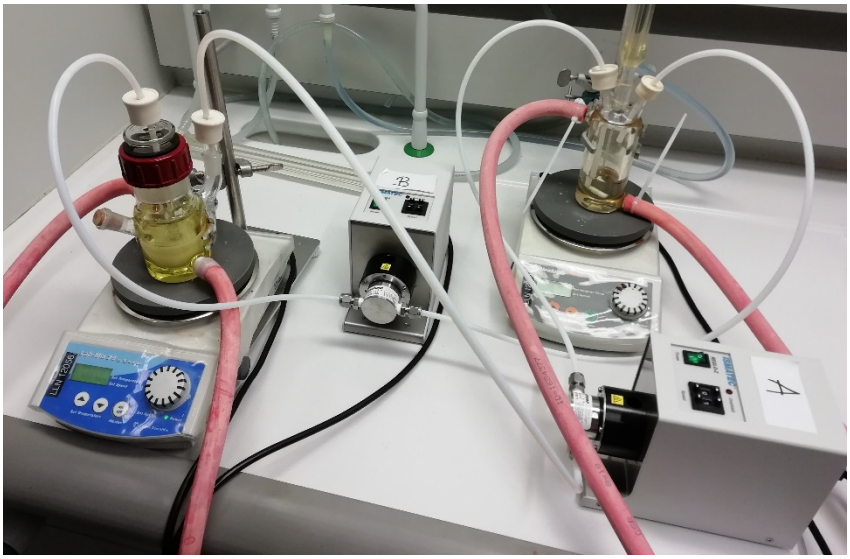

Figure 3 Real-view image of the deracemization set-up. Red tubing are for the heating or cooling liquids while white PTFE tubing is used for the solution transfer. On the left, one can see the crystallization vessel with solid in suspension and on the right the racemization vessel with a clear solution inside.

4.2 Experiment n°1

Conditions: 5g of RS-BnFTP, 2.98g of S-PBA (1eq), 90mL of toluene, 203µL of DBU (0.075eq), $T_{racemization}$ = 60-90°C, $T_{crystallization}$ = 10-15°C. The speed of the pumps is variable over the experiment. The speed is normally taken as the lowest possible (4.2mL/min) but due to a difference in the strains for the two pumps, the speed of the liquid being pumped from the crystallization vessel differs from the one pumped from the racemization vessel. The crystallization vessel was stirred at 1000rpm while the racemization vessel was stirred at 400rpm. The system was equilibrated with all the components except DBU for 1h30 in order to have the imbalance in solution. Then the pumps were turned off and DBU was added in the racemization vessel. Both vessel stirred for 4h then the pumps were turned on again. One sample was taken from the racemization vessel prior to DBU addition (sample A0) and after 3h45 (sample A1). The pumps ran for 2h30 and were turned off again for the night. The temperature of the racemization vessel was decreased to 60°C for the night. The morning after at 9h38, the pumps were turned on and the racemization vessel put back at 90°C. At 11h08, the pumps were turned off again for 3h45. 2 samples were taken, one at 11h08 (sample B0) and one 3h45 later (sample B1). Then the pumps were turned on until 6pm and off for the night, the racemization vessel was kept at 90°C. The morning after, a sample was taken at 10h (sample B2) and the pumps were turned on again. At 11h40, the crystallization vessel was brought down to 10°C. At 14h20, a sample was taken from the racemization vessel (sample C0) and the pumps were turned for the night at 5pm. The morning after, a sample was taken at 9h40 (sample C1) and the pumps restarted. At 3pm, the racemization vessel was pumped back to the crystallization vessel and the pumps were turned off. The crystallization was kept stirring at 10°C for 1h30 and the suspension was filtered over büchner.

	$ee_{racemization\ vessel}$
Sample A0	0,32[R]
Sample A1	0,00
Sample B0	0,22[R]
Sample B1	0,14[R]
Sample B2	0,01[R]
Sample C0	0,24[R]
Sample C1	0,06[S]

Table 4 Enantiomeric excess of the racemization vessel over the course of the deracemization process (run 1)

4.3 Experiment n°2

Conditions: 6.25g of RS-BnFTP, 3.73g of R-PBA (1eq), 90mL of toluene, 254µL of DBU (0.075eq), $T_{racemization}$ = 70-90°C, $T_{crystallization}$ = 10°C. The speed of the pumps is variable over the experiment. The speed is normally taken as the lowest possible (4.2mL/min) but due to a difference in the strains for the two pumps, the speed of the liquid being pumped from the crystallization vessel differs from the one pumped from the racemization vessel. The crystallization vessel was stirred at 600rpm while the racemization vessel was stirred at 400rpm. The system was equilibrated with all the components except DBU for 1h00 in order to have the imbalance in solution. Then the pumps were turned off and DBU was added in the racemization vessel. Both vessel stirred for 3h30 then the pumps were turned on again. One sample was taken from both the crystallization and the racemization vessel prior to DBU addition and after 3h30. Then samples were taken at different moment during the 2 first days of run. I must be noted that the sample from the crystallization vessel was taken out of the pomp that brings the liquid from the crystallization vessel to the racemization (to avoid having solid in suspension). At night, the heating was

decreased to 70°C and the pumps turned off. On day 5 of run, at 3pm, the racemization vessel was pumped back to the crystallization vessel and the pumps were turned off. The crystallization was kept stirring at 5°C for 1h00 and the suspension was filtered over büchner.

Sample Number	Sample Name	$ee_{Crystallization\ vessel}$	$ee_{Racemization\ vessel}$
D1.1	Day 1 11h15	0.54 [S]	0.20 [R]
D1.2	Day 1 14h45	0.08 [R]	0
D1.3	Day 1 15h45	0.02 [S]	0.05 [S]
D1.4	Day 1 16h45	0.34 [R]	0.30 [R]
D1.5	Day 1 17h45	0.25 [R]	0.04 [S]
D1.6	Day 1 18h45	0.33 [R]	0.04 [R]
D2.1	Day 2 9h30	0.25 [S]	0.13 [R]
D2.2	Day 2 10h30	0	0.02 [R]
D2.3	Day 2 11h30	0.34 [R]	0.02 [R]
D2.4	Day 2 14h30	0.04 [R]	0.04 [S]

Table 5 Enantiomeric excess of both the crystallization and racemization vessel over the first two days of the deracemization process (run 2)

4.4 Experiment n°3

Conditions: 7.5g of RS-BnFTP, 4.47g of R-PBA (1eq), 90mL of toluene, 305µL of DBU (0.075eq), $T_{racemization}$ = 75°C, $T_{crystallization}$ = 10°C. The speed of the pumps is variable over the experiment. The speed is normally taken as the lowest possible (4.2mL/min) but due to a difference in the strains for the two pumps, the speed of the liquid being pumped from the crystallization vessel differs from the one pumped from the racemization vessel. The crystallization vessel was stirred at 600rpm while the racemization vessel was stirred at 400rpm. The process ran for 5 days and at night, the pumps were off and heating too. Most of the liquid was transferred to the crystallization vessel. At 3pm, the racemization vessel was pumped back to the crystallization vessel and the pumps were turned off. The crystallization was kept stirring at 0°C for 1h00 and the suspension was filtered over büchner.

5. HPLC chromatograms

5.1 Enantiomeric excess of BnFTP with the acid when heating is applied

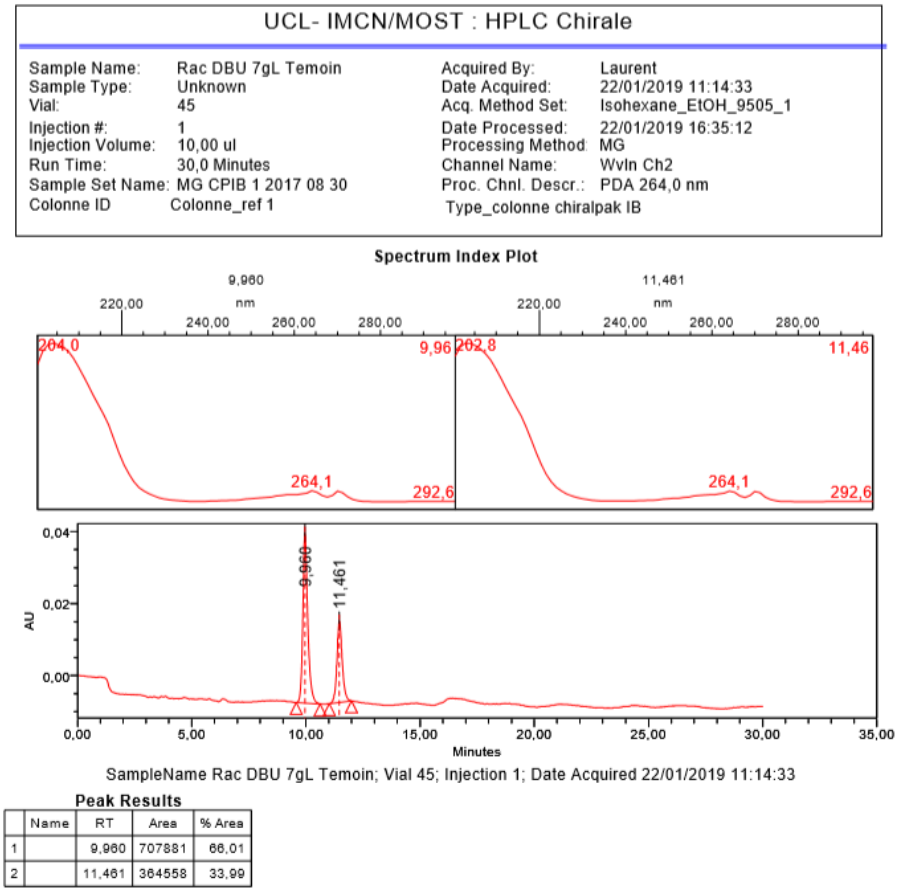

Figure 4 Chromatogram of the starting mixture to racemize at 110°C in toluene

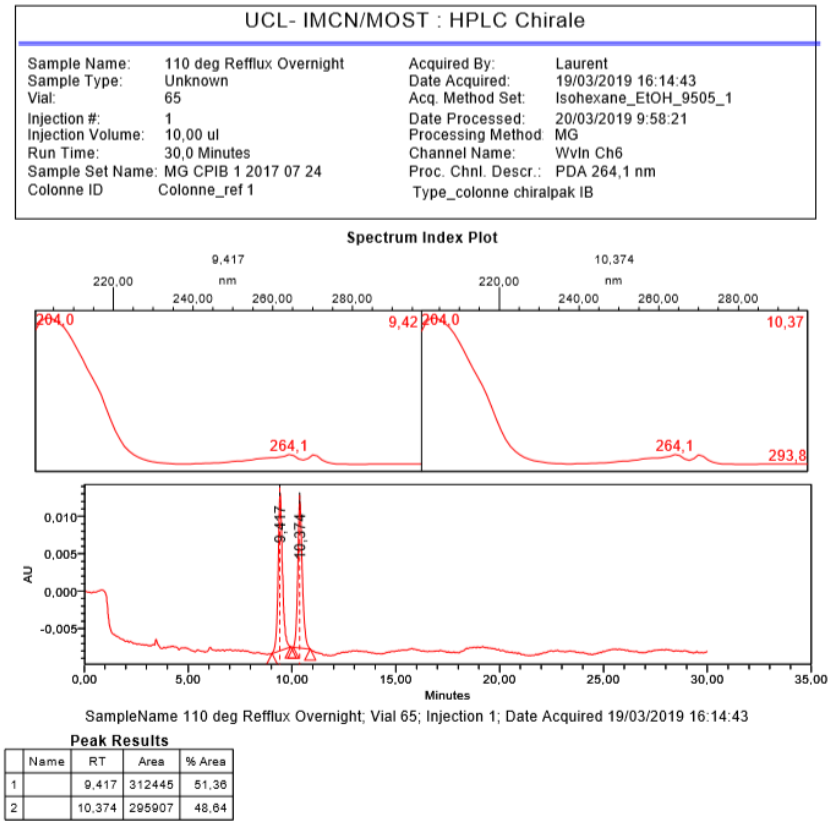

Figure 5 Chromatogram of the mixture obtained after 12h at 110°C in toluene

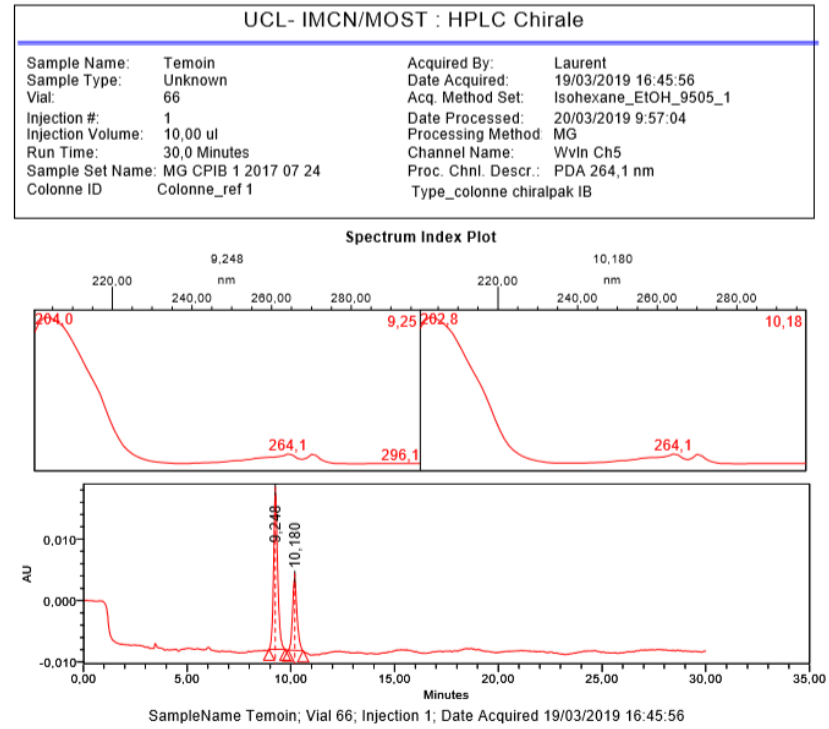

Peak Results

	Name	RT	Area	% Area
1		9,248	348807	66,76
2		10,180	173638	33,24

Figure 6 Chromatogram of the starting mixture to racemize at 90°C in toluene

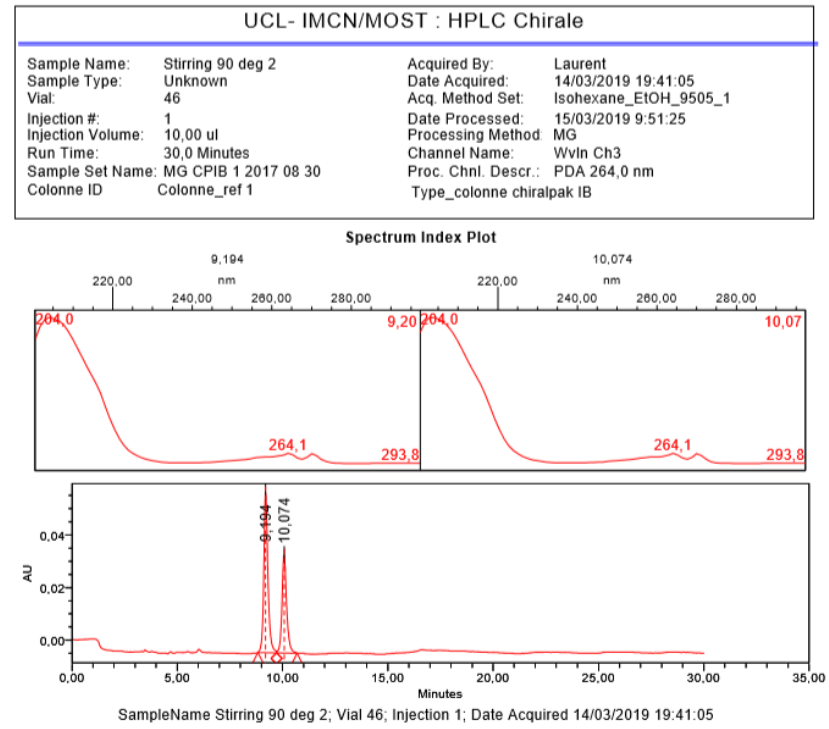

Peak Results

	Name	RT	Area	% Area
1		9,194	840119	59,61
2		10,074	569164	40,39

Figure 7 Chromatogram of the mixture after 2h at 90°C in toluene

5.2 Deracemization n°1

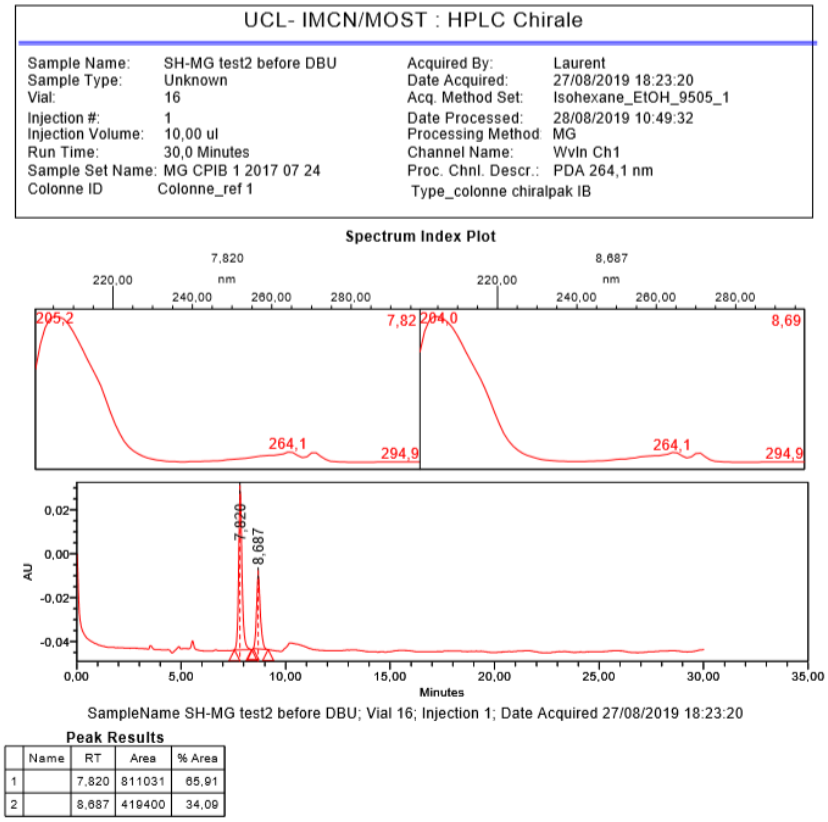

Figure 8 Chromatogram of sample A0

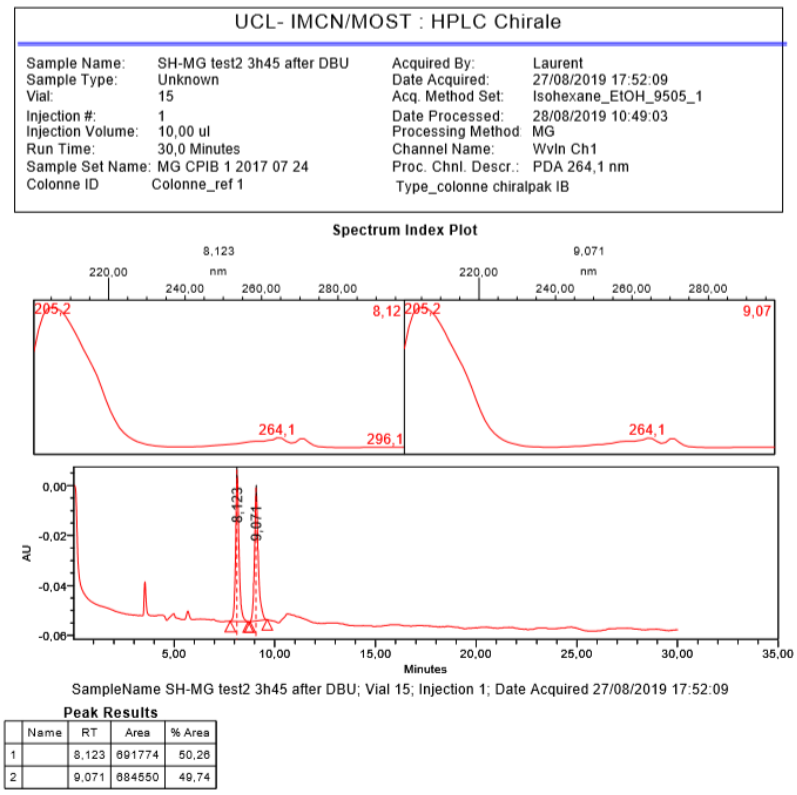

Figure 9 Chromatogram of sample A1

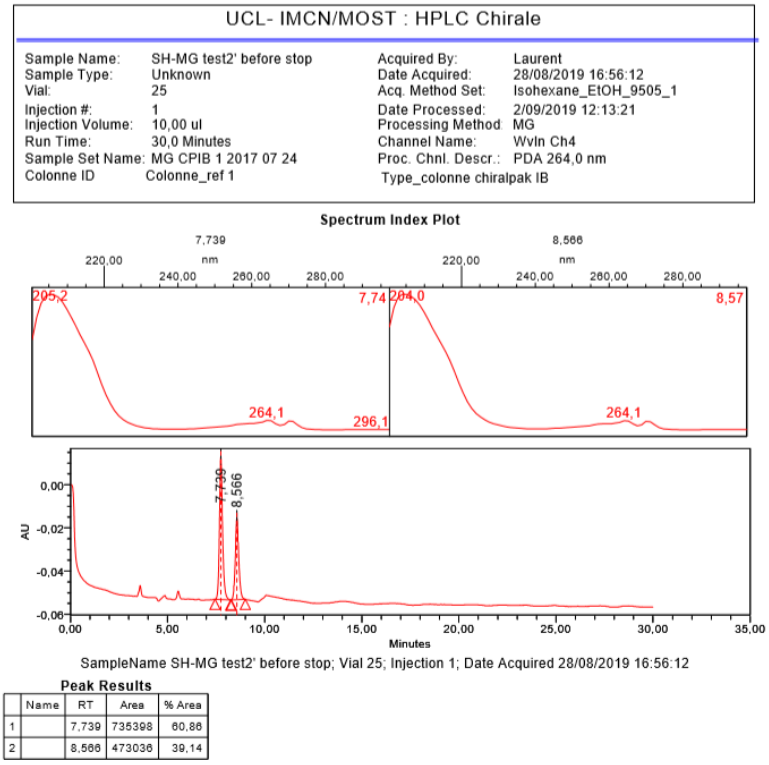

Figure 10 Chromatogram of sample B0

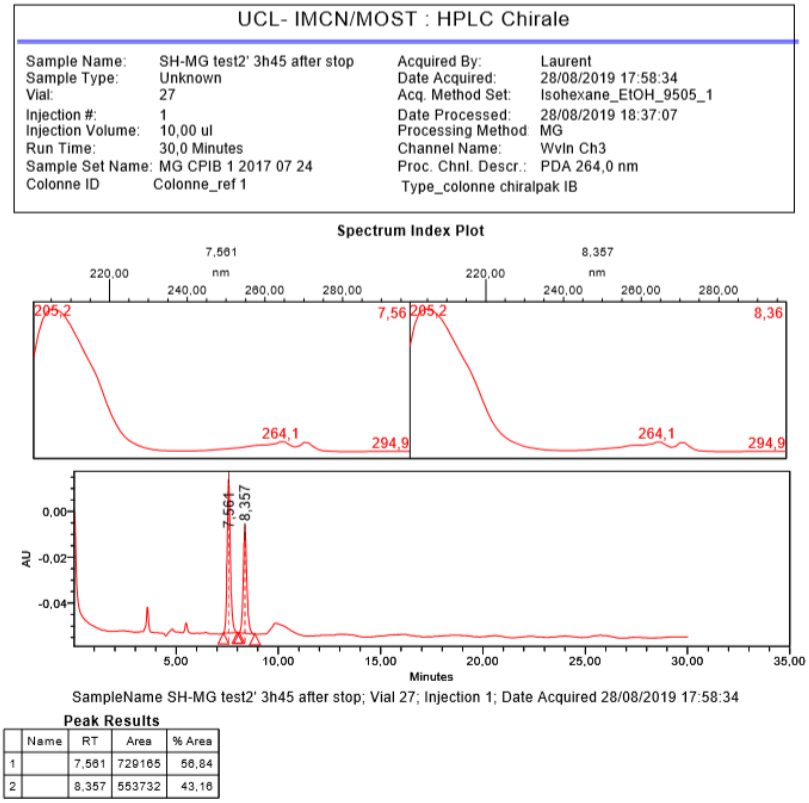

Figure 11 Chromatogram of sample B1

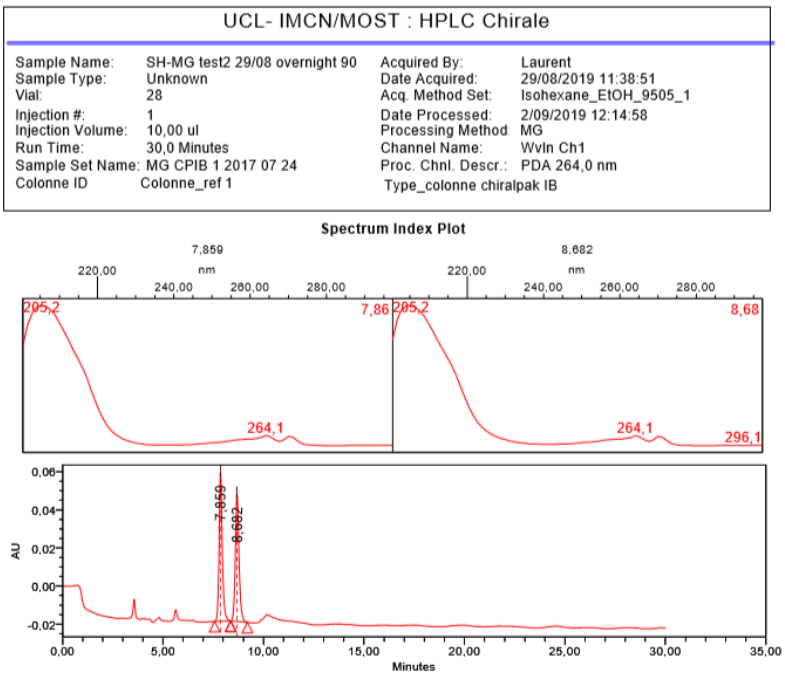

Peak Results

	Name	RT	Area	% Area
1		7,859	867649	50,58
2		8,682	847745	49,42

Figure 12 Chromatogram of sample B2

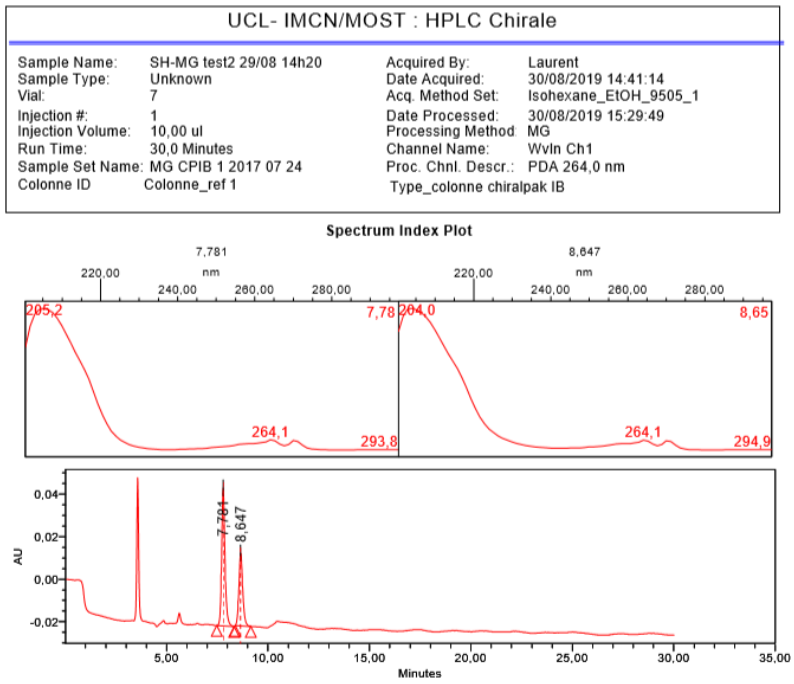

Peak Results

	Name	RT	Area	% Area
1		7,781	737103	62,12
2		8,647	449472	37,88

Figure 13 Chromatogram of sample C0

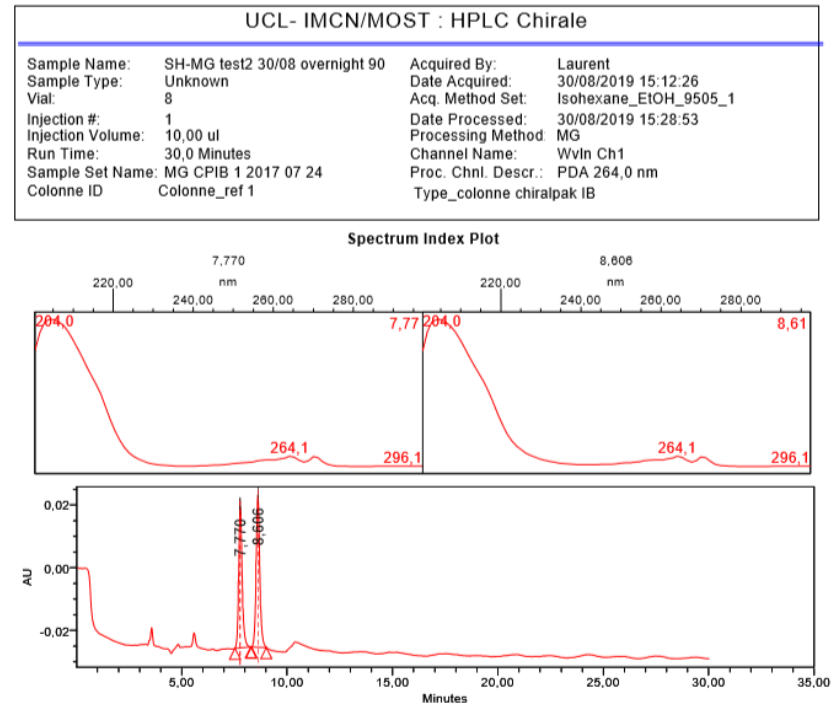

Figure 14 Chromatogram of sample C1

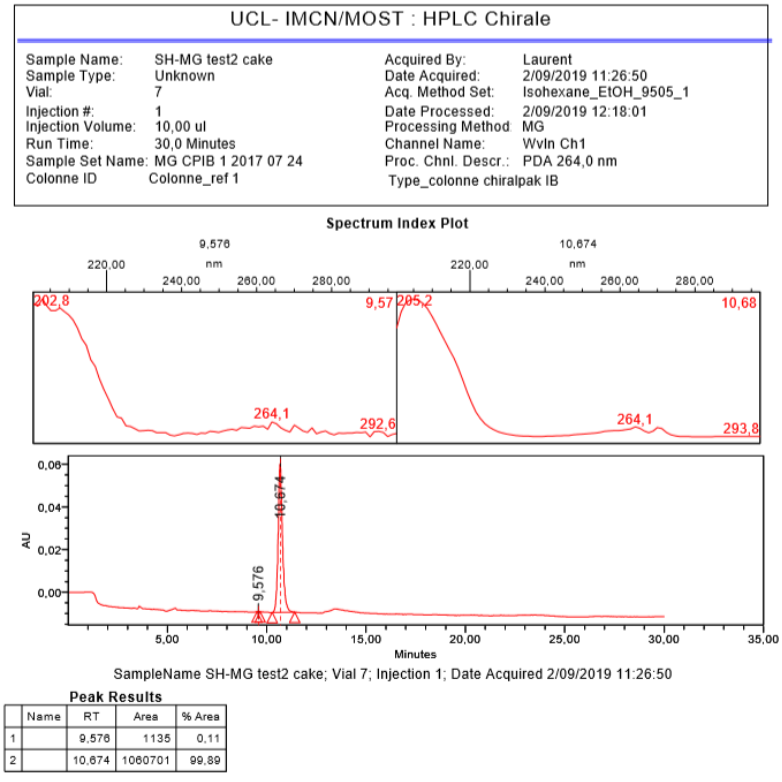

Figure 15 Chromatogram of the filtrate (experiment 1)

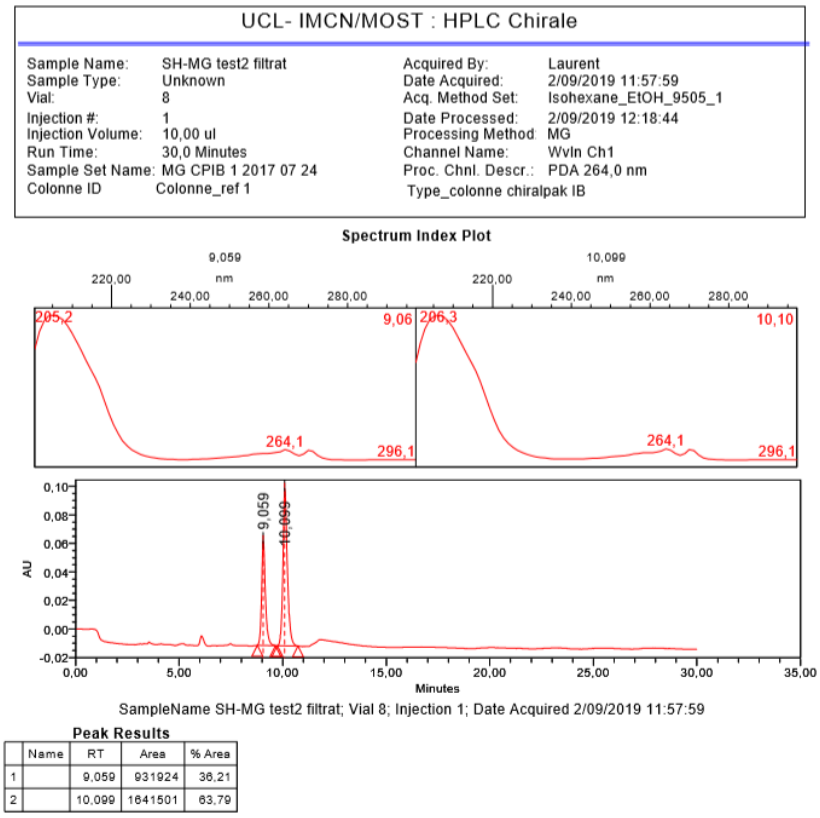

Figure 16 Chromatogram of the cake (experiment 1)

5.3 Deracemization n°2

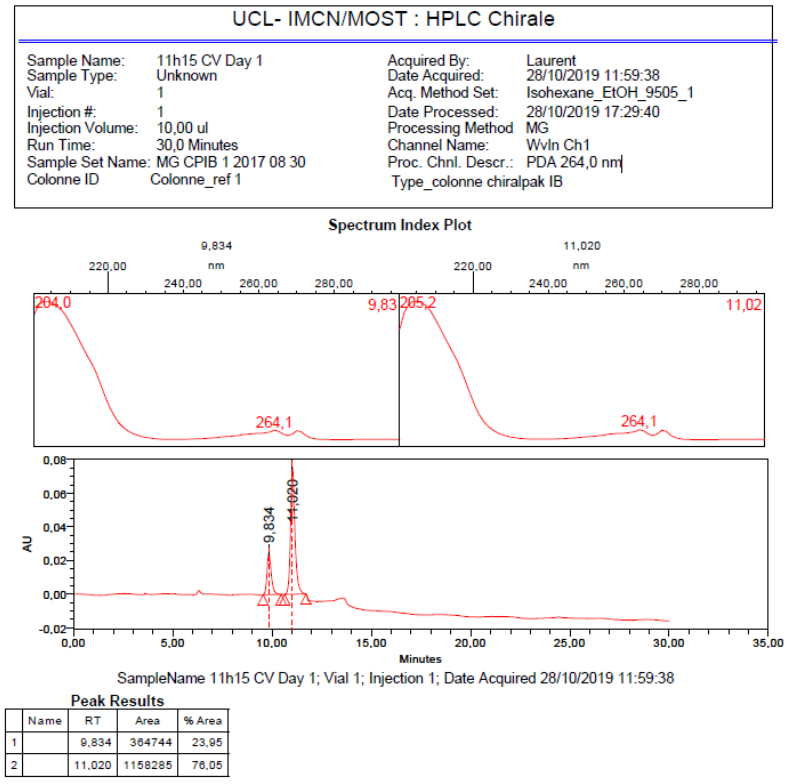

Figure 17 Chromatogram of sample D1.1 (crystallization vessel)

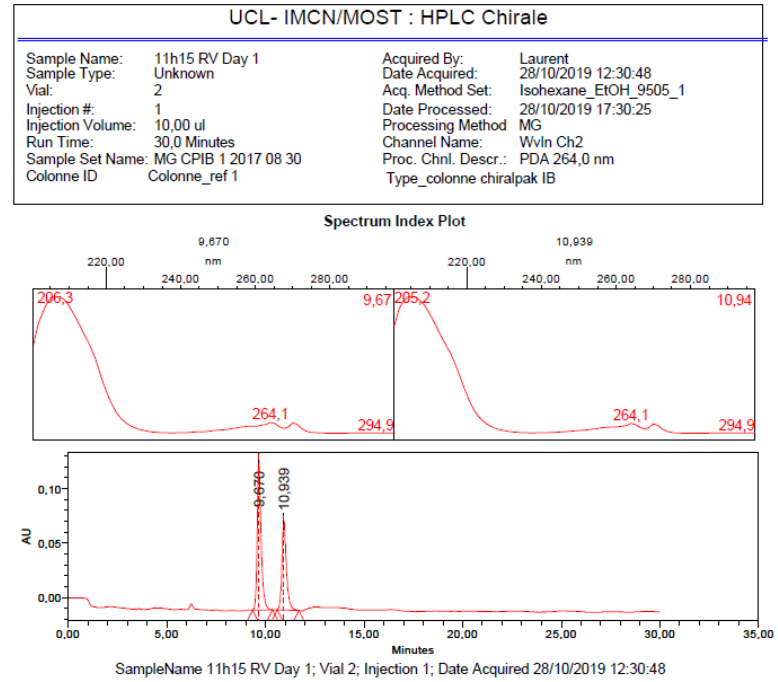

Figure 18 Chromatogram of sample D1.1 (Racemization vessel)

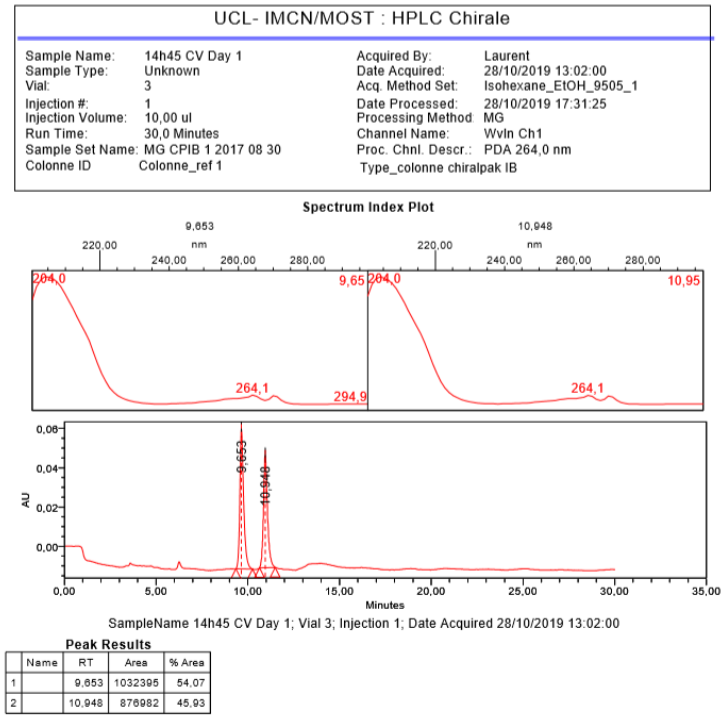

Figure 19 Chromatogram of sample D1.2 (Crystallization vessel)

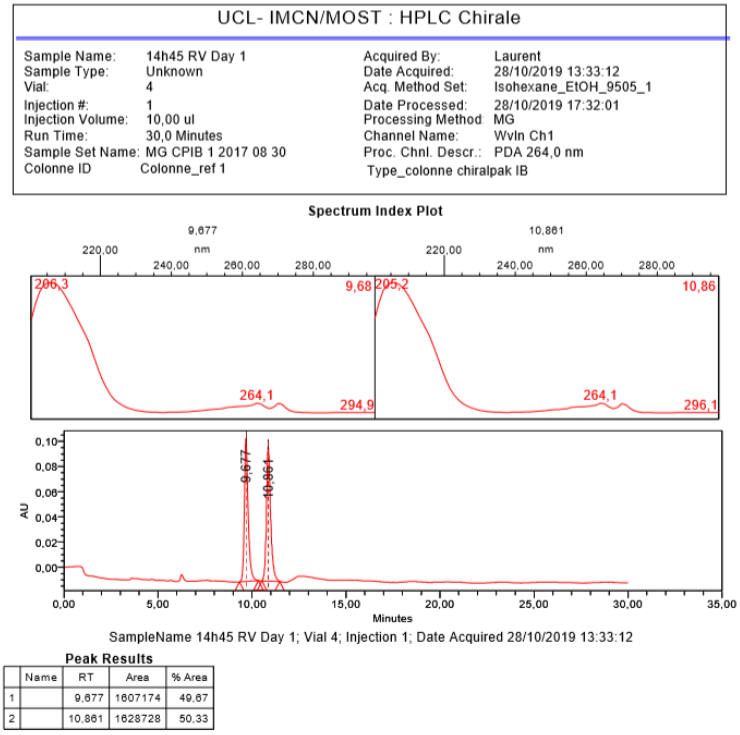

Figure 20 Chromatogram of sample D1.2 (Racemization vessel)

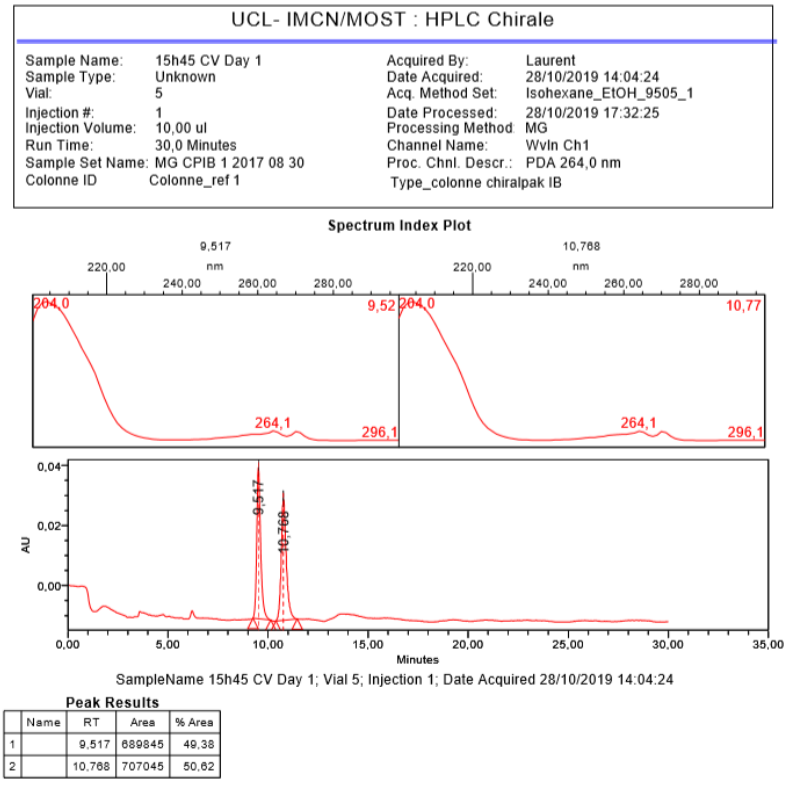

Figure 21 Chromatogram of sample D1.3 (Crystallization vessel)

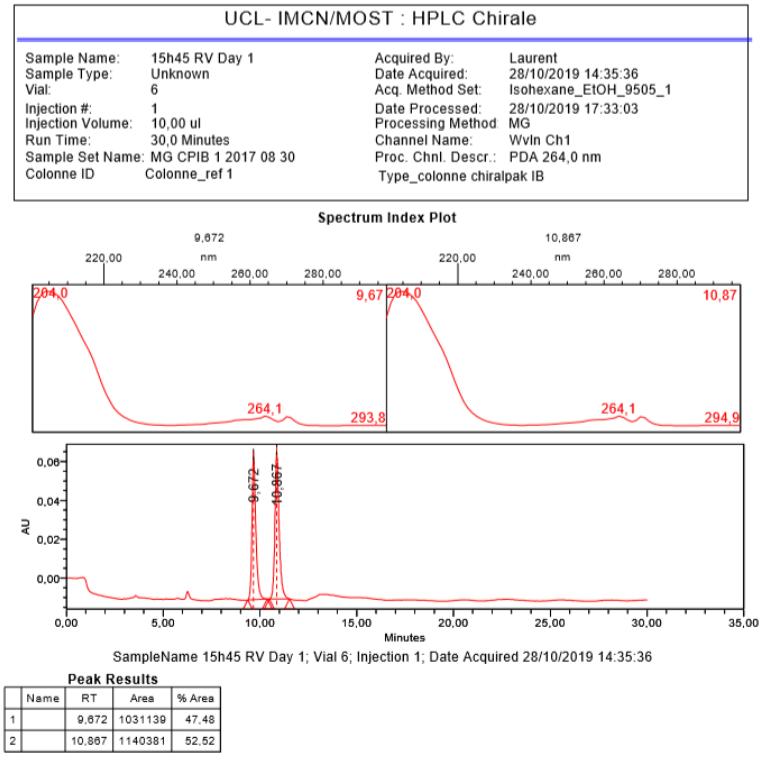

Figure 22 Chromatogram of sample D1.3 (Racemization vessel)

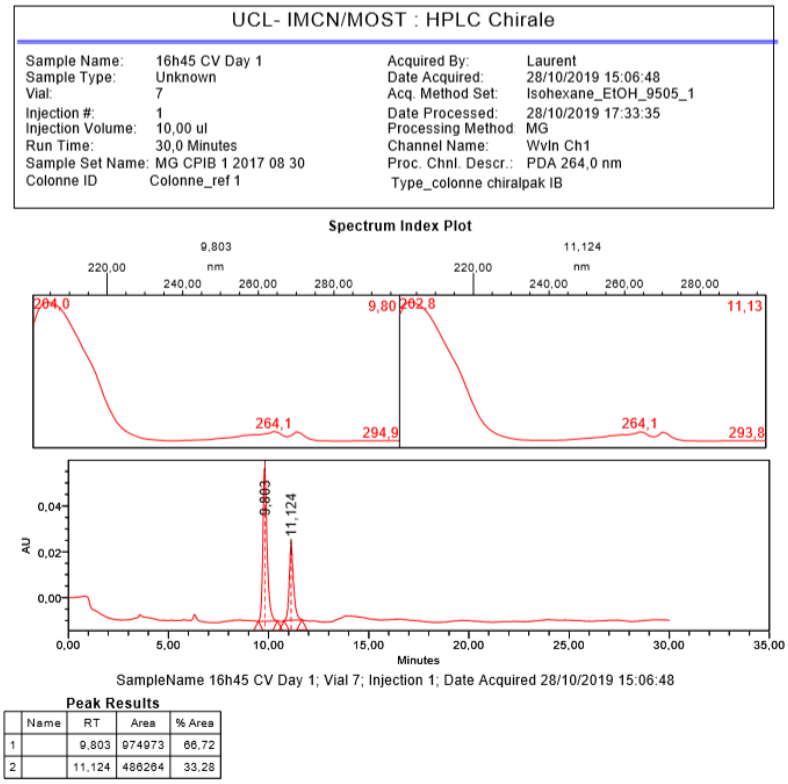

Figure 23 Chromatogram of sample D1.4 (Crystallization vessel)

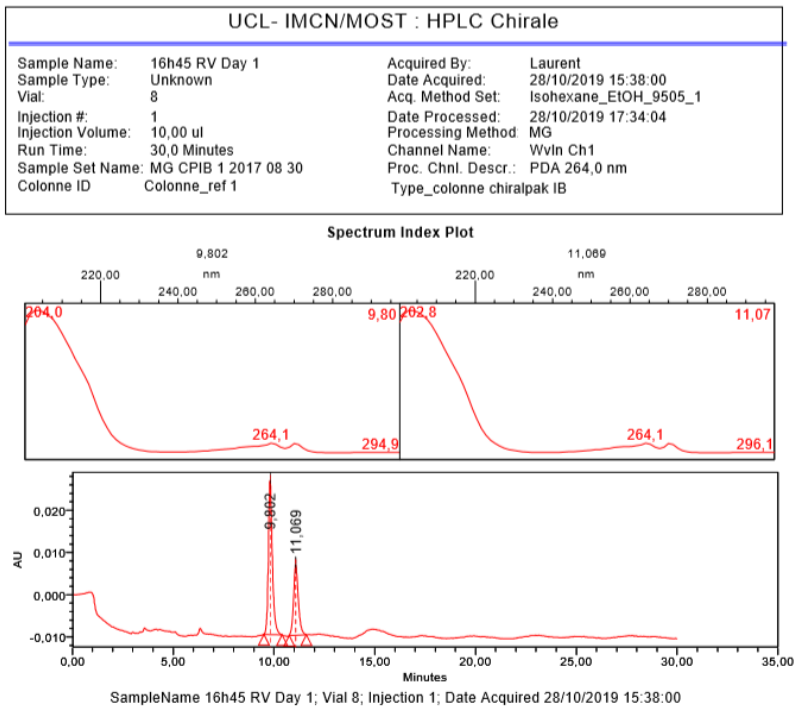

Figure 24 Chromatogram of sample D1.4 (Racemization vessel)

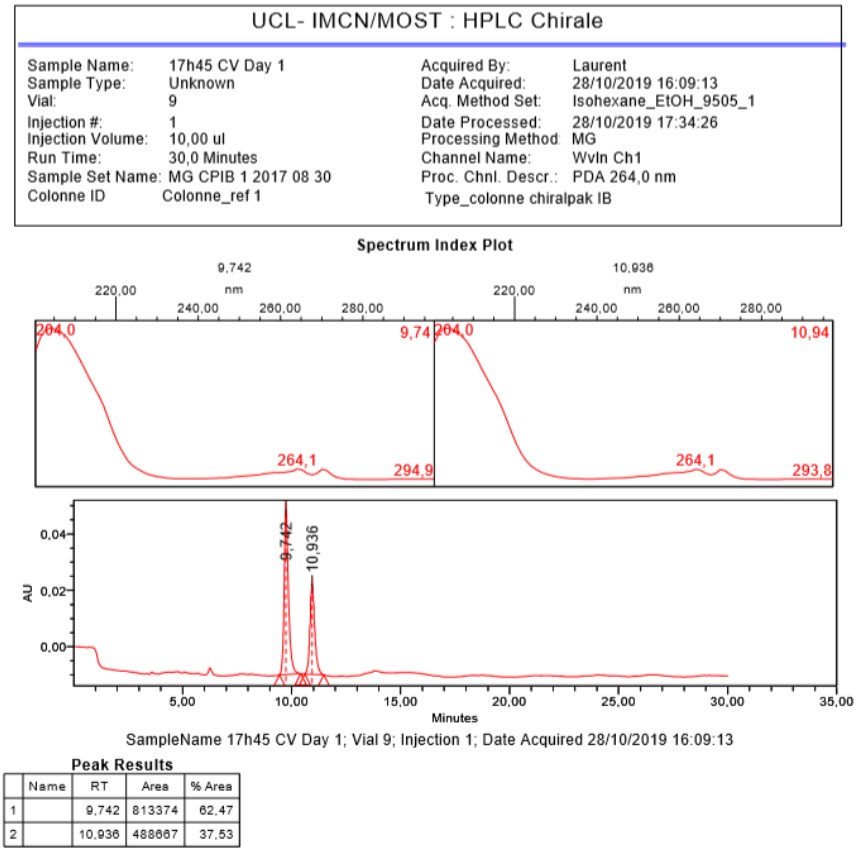

Figure 25 Chromatogram of sample D1.5 (Crystallization vessel)

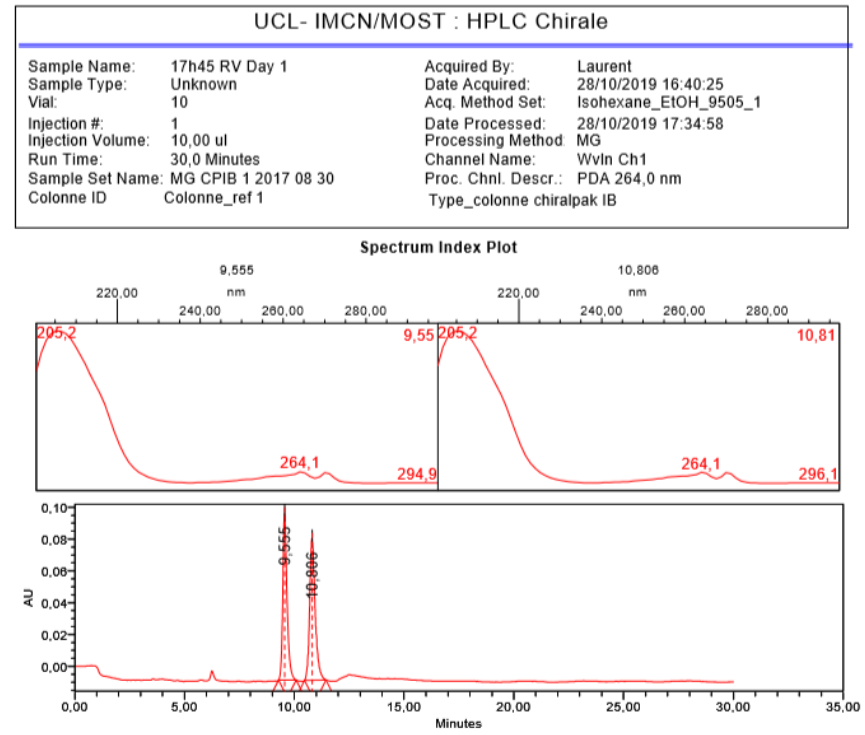

Figure 26 Chromatogram of sample D1.5 (Racemization vessel)

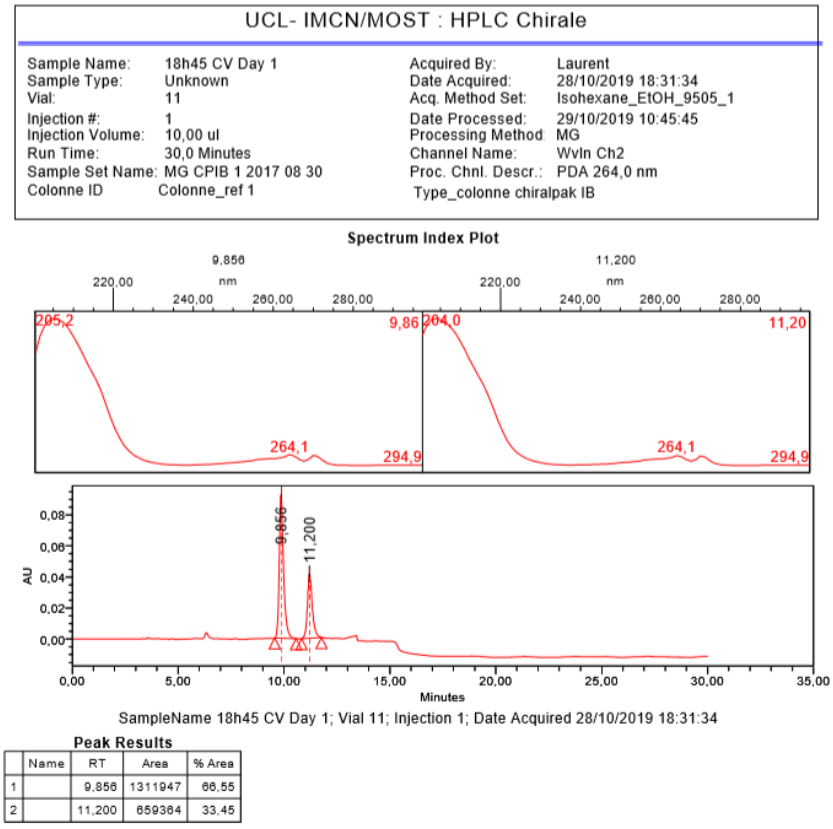

Figure 27 Chromatogram of sample D1.6 (Crystallization vessel)

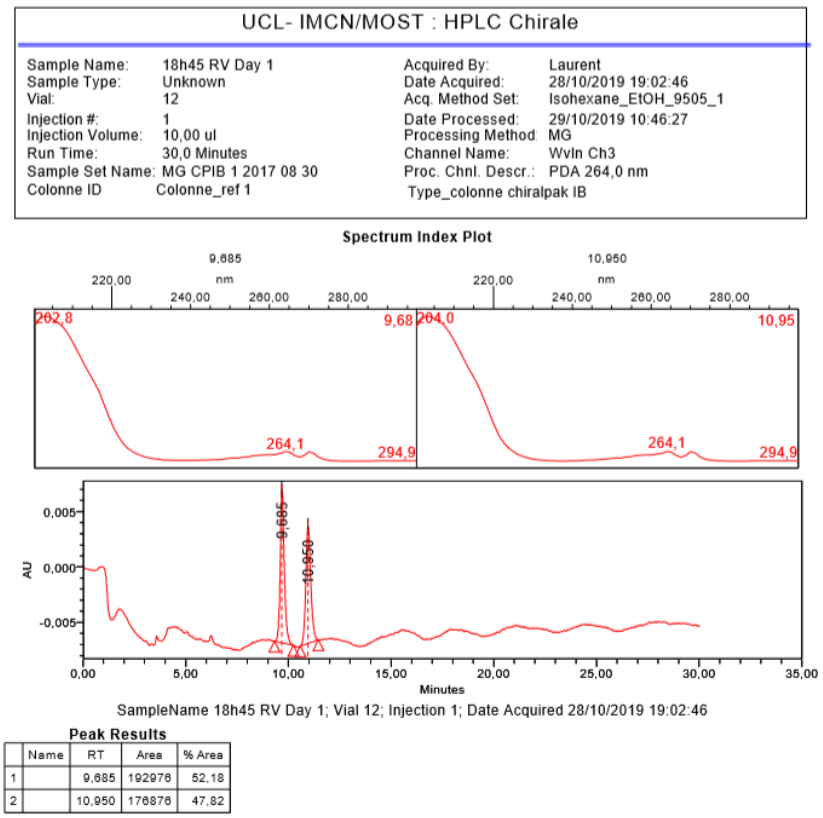

Figure 28 Chromatogram of sample D1.6 (Racemization vessel)

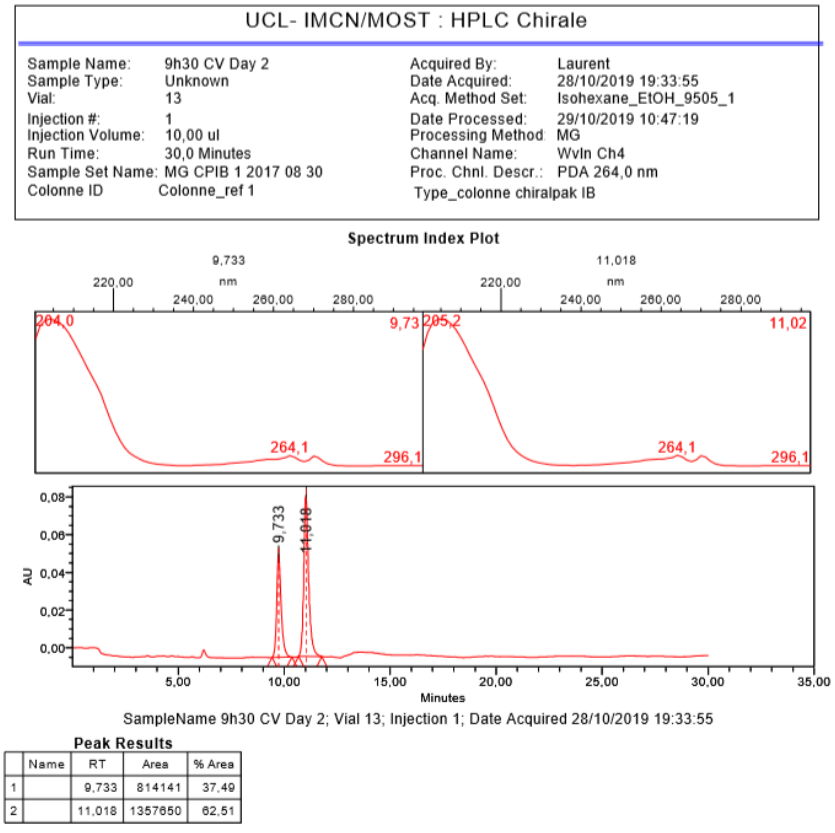

Figure 29 Chromatogram of sample D2.1 (Crystallization vessel)

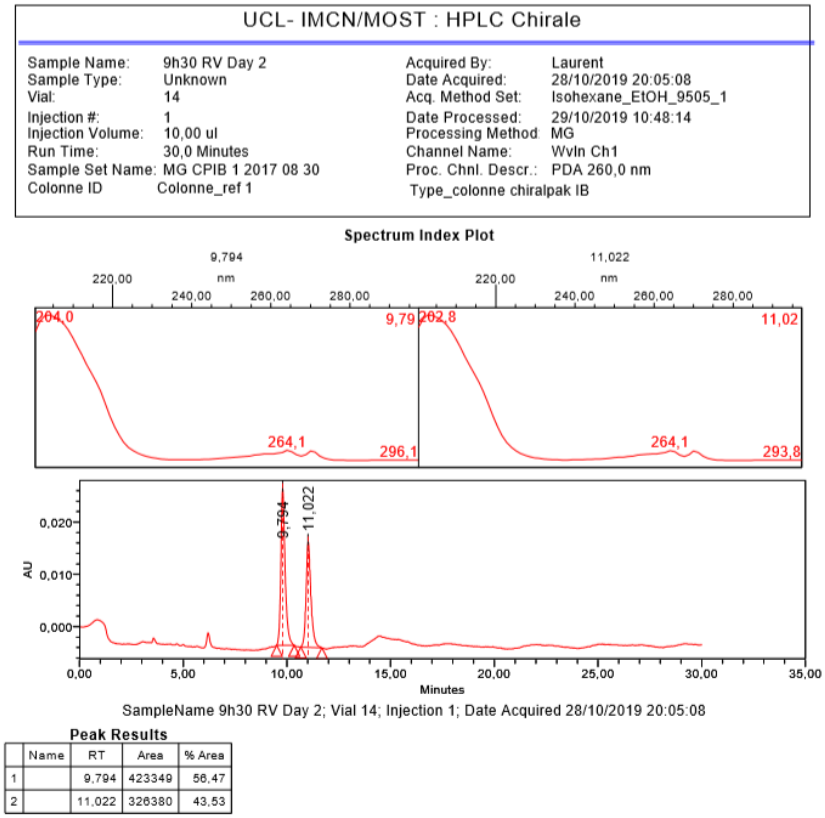

Figure 30 Chromatogram of sample D2.1 (Racemization vessel)

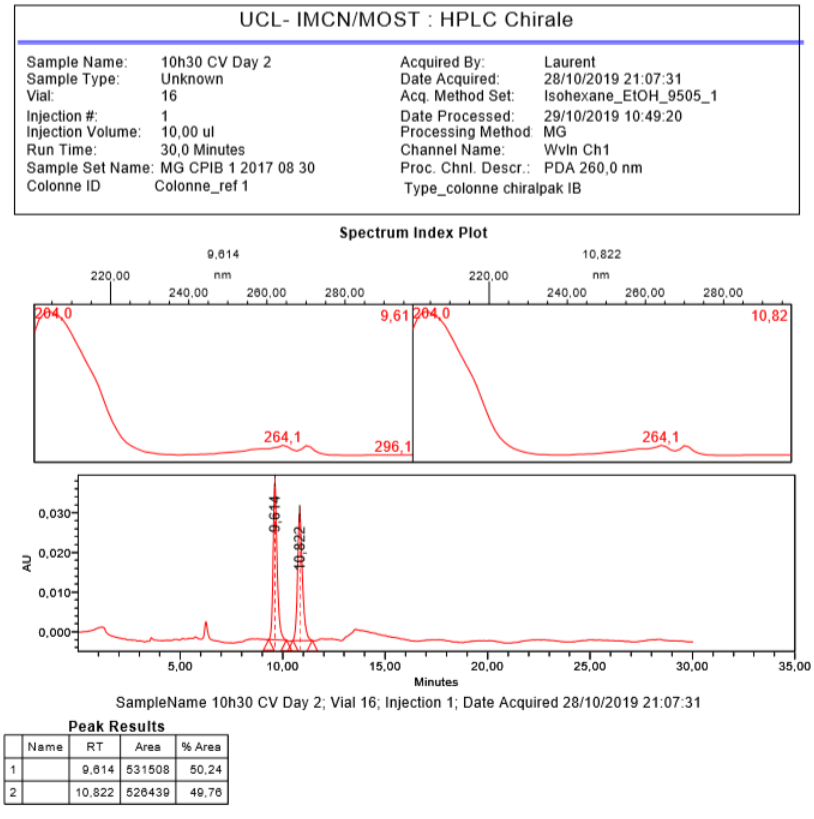

Figure 31 Chromatogram of sample D2.2 (Crystallization vessel)

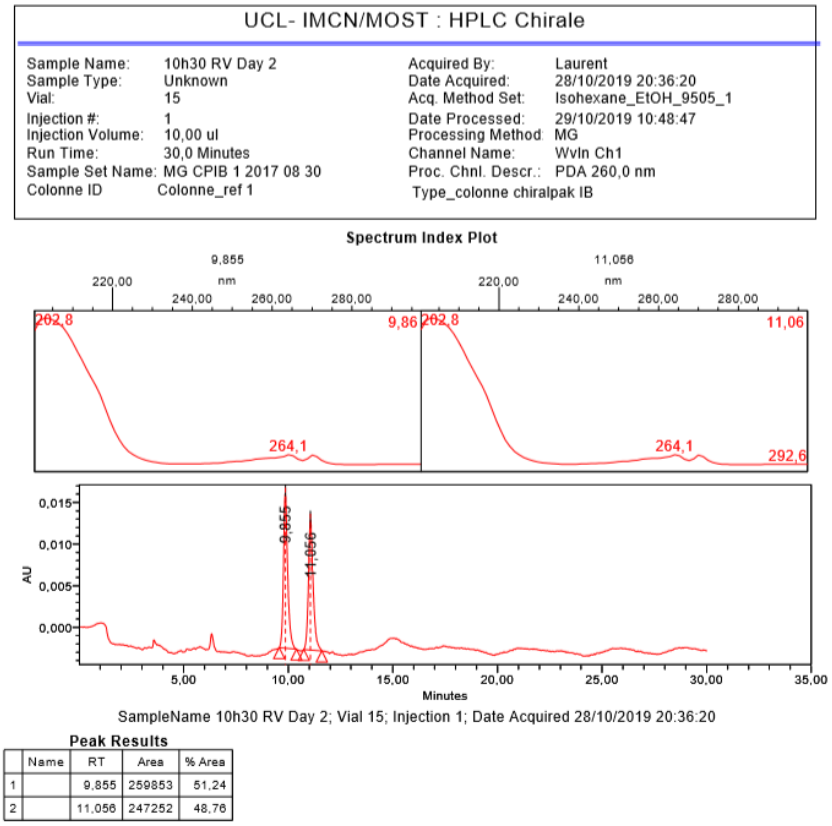

Figure 32 Chromatogram of sample D2.2 (Racemization vessel)

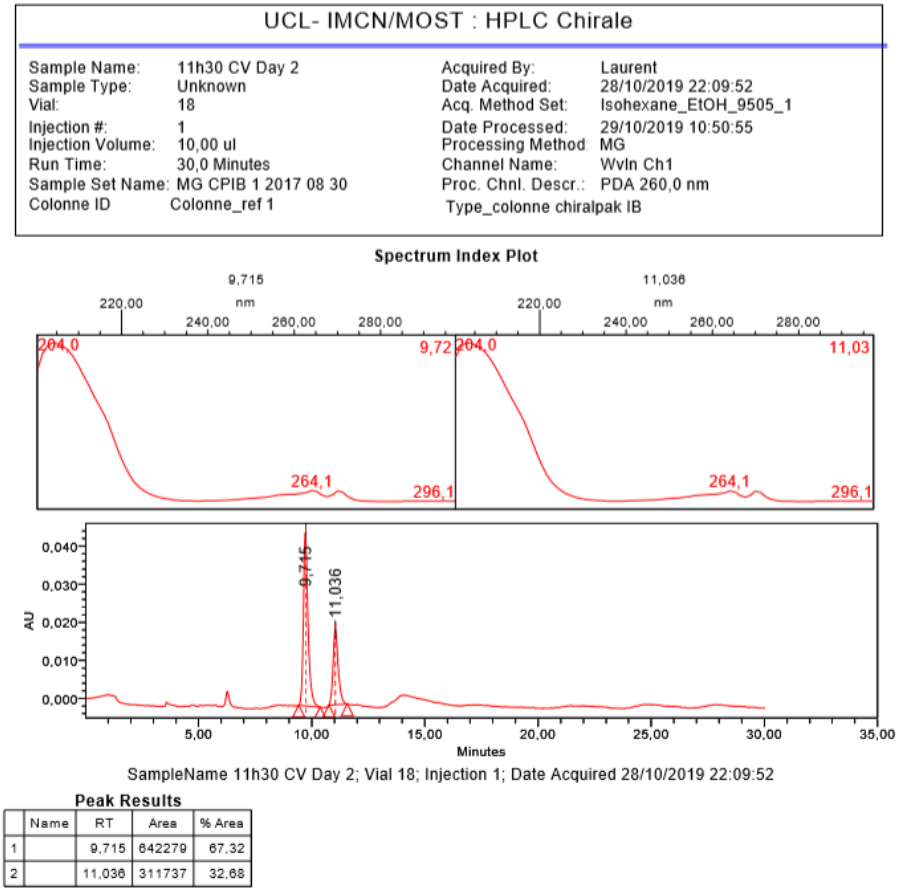

Figure 33 Chromatogram of sample D2.3 (Crystallization vessel)

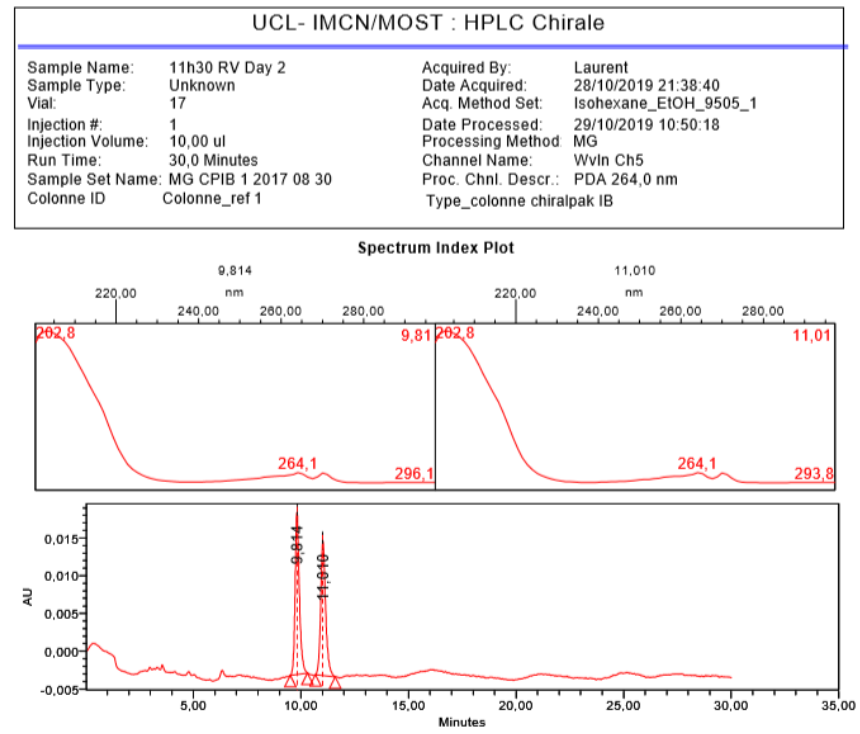

Peak Results

	Name	RT	Area	% Area
1		9,814	300673	51,30
2		11,010	285455	48,70

Figure 34 Chromatogram of sample D2.3 (Racemization vessel)

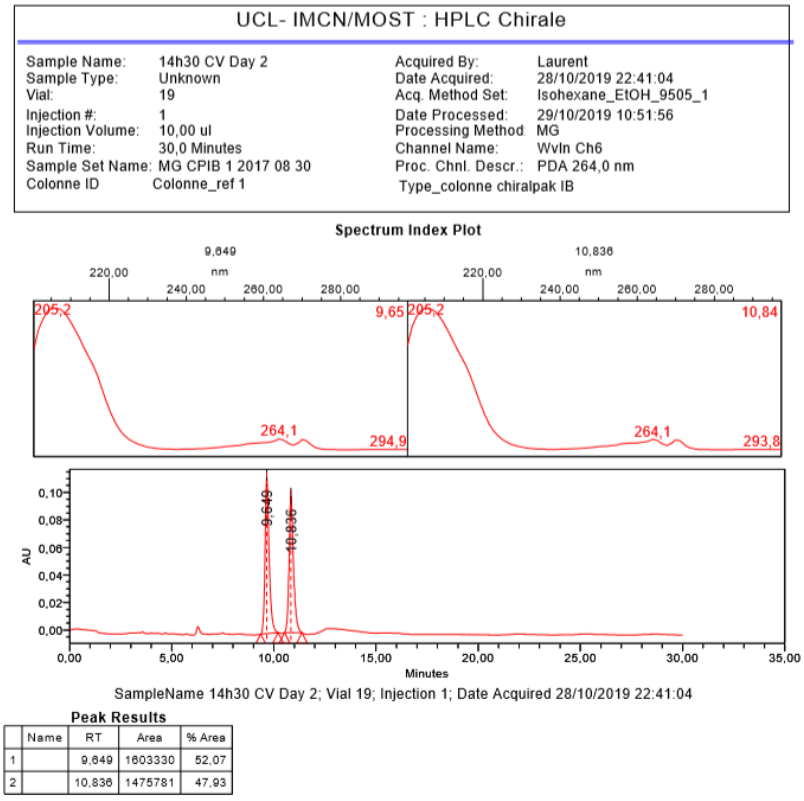

Peak Results

	Name	RT	Area	% Area
1		9,649	1603330	52,07
2		10,836	1475781	47,93

Figure 35 Chromatogram of sample D2.4 (Crystallization vessel)

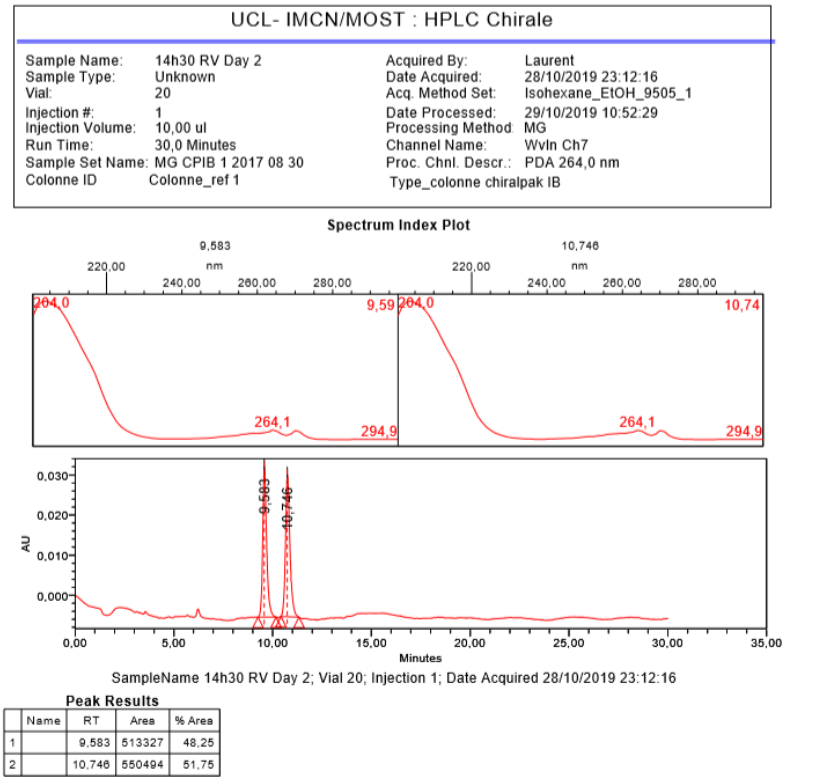

	Name	RT	Area	% Area
1		9,583	513327	48,25
2		10,746	550494	51,75

Figure 36 Chromatogram of sample D2.4 (Racemization vessel)

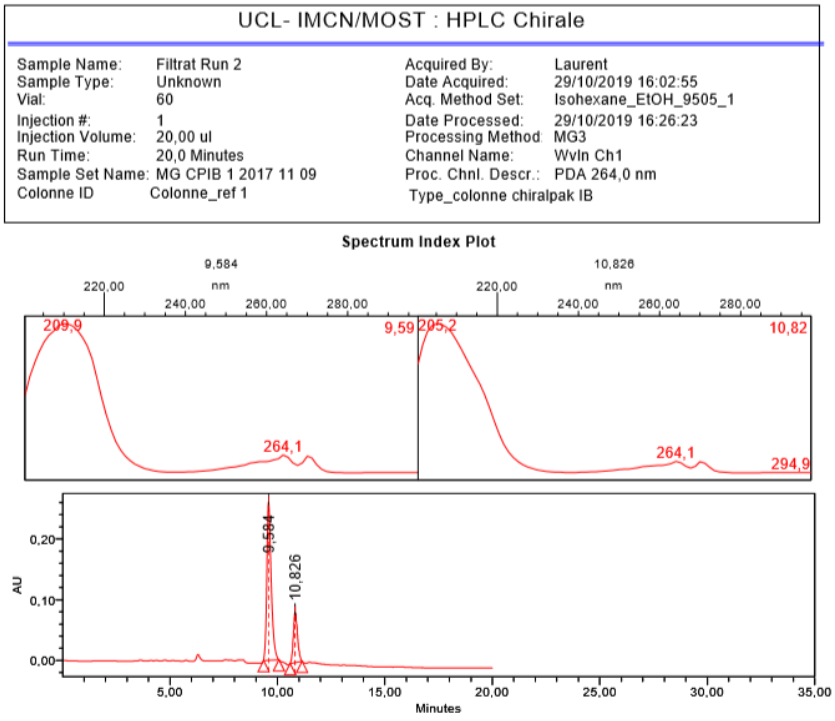

	Name	RT	Area	% Area
1		9,584	3698691	77,06
2		10,826	1101150	22,94

Figure 37 Chromatogram of the filtrate (experiment 2)

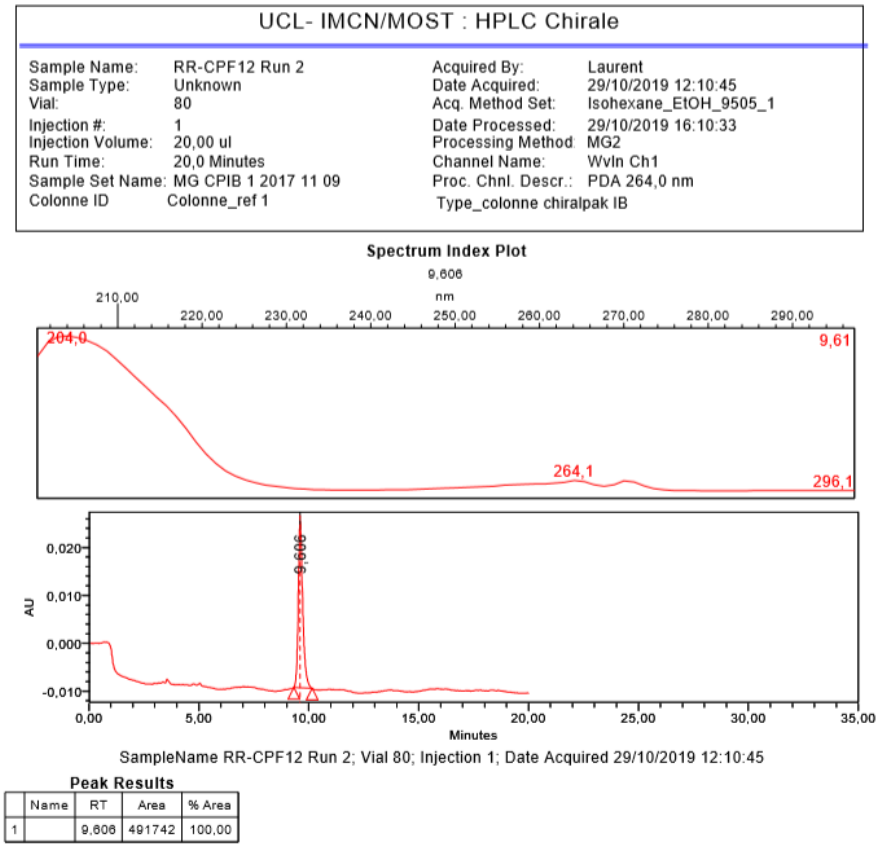

Figure 38 Chromatogram of the cake (experiment 2)

7.7 Deracemization n°3

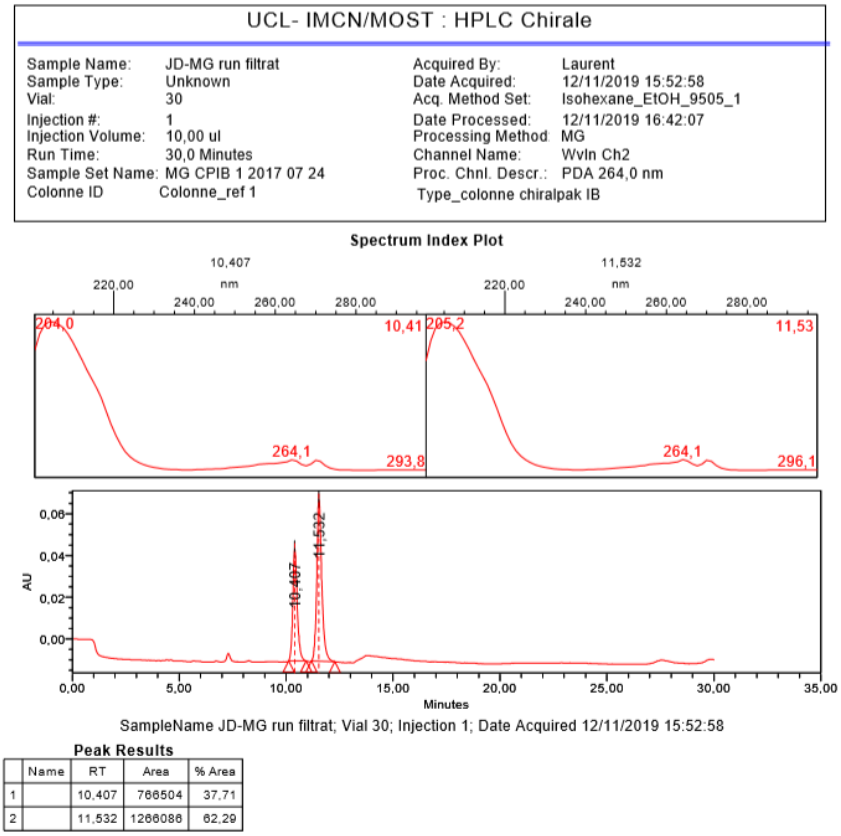

Figure 39 Chromatogram of the filtrate (experiment 3)

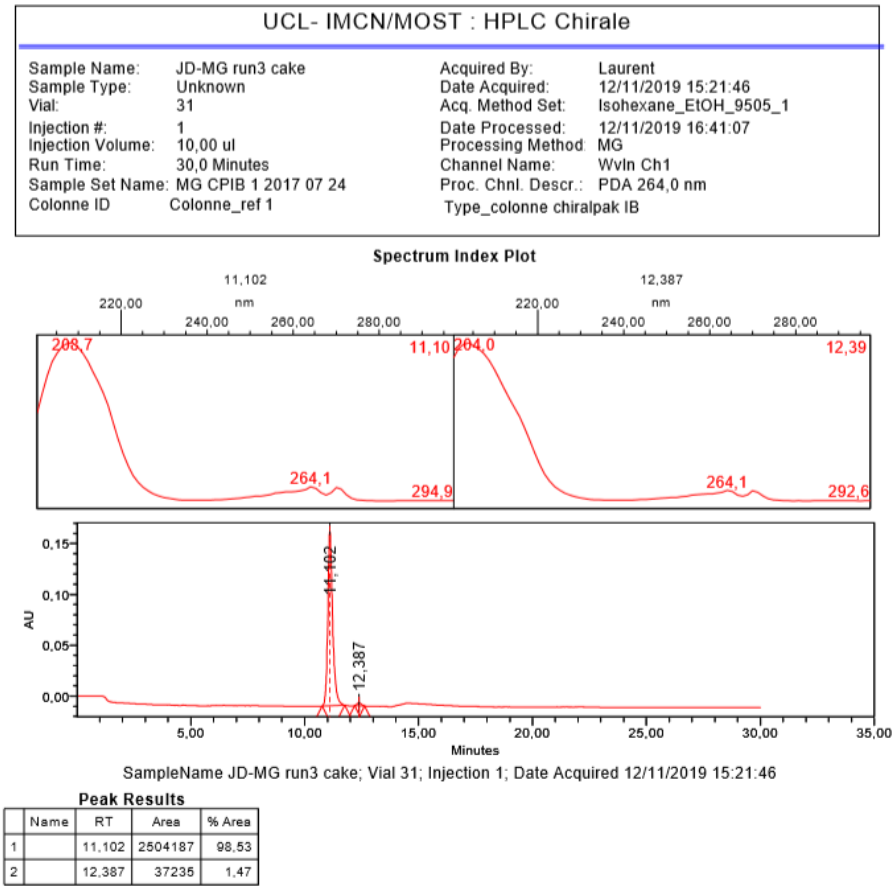

Figure 40 Chromatogram of the cake (experiment 3)